电 化 学
J. Electrochem. 2022, 28(11), 2219012 (1 of 23)

[Review] DOI: 10.13208/j.electrochem.2219012 http://electrochem.xmu.edu.cn

Which Factor Dominates Battery Performance: Metal Ion Solvation Structure-Derived Interfacial Behavior or Solid Electrolyte Interphase Layer?

Hao-Ran Cheng[1,2], Zheng Ma[1], Ying-Jun Guo[3], Chun-Sheng Sun[3], Qian Li[1], Jun Ming[1,2*]

(*1. State Key Laboratory of Rare Earth Resource Utilization Changchun Institute of Applied Chemistry, Chinese Academy of Sciences, Changchun 130022, Jilin, China; 2. School of Applied Chemistry and Engineering University of Science and Technology of China, Hefei 230026, Anhui, China; 3. Huzhou Kunlun Enchem Battery Materials Co., Ltd., Huzhou 313103, Zhejiang, China.*)

Abstract: Solid-electrolyte interphase (SEI) layer formed on the electrode by electrolyte decomposition has been considered to be one of the most important factors affecting the battery performance. We discover that the metal ion solvation structure can also influence the performance, particularly, it can elucidate many phenomena that the SEI cannot. In this review, we summarize the importance of the metal ion solvation structure and the derived metal ion de-solvation behaviors, by which we can build an interfacial model to show the relationship between the interfacial behavior and electrode performance, and then apply to different electrode and battery systems. We emphasize the influences of ionic and molecular interactions on electrode surface that differ from previous SEI-based interpretations. This review provides a new view angle to understand the battery performance and guide the electrolyte design.

Key words: battery; electrolyte; solvation structure; electrode interfacial model; solid electrolyte interphase layer

1 Introduction

Metal ion batteries have become the most appealing energy storage and conversion technology in portable electronic devices and electric vehicles (EVs) due to their high energy density, long lifespan, and environmental sustainability[1-4]. To improve the battery performances, engineering the solid electrolyte interphase (SEI) that is formed on the electrode surface by tuning electrolyte decomposition has become the most commonly used strategy in practical application[5-9], as the formed SEI is considered to be effective for stabilizing the electrode and electrolyte. This viewpoint is popular and has become the main principle for guiding the electrolyte design, such as in the development of lithium-ion batteries (LIBs) in the past two decades[10-21]. The most successful case is the utilization of ethylene carbonate (EC)-based electrolyte instead of propylene carbonate (PC)-based electrolyte, as a good SEI can be formed on the carbon-based anode by the decomposition of EC solvent, enabling a reversible Li^+ (de-)intercalation within carbon layers[22]. This discovery enabled the final commercialization of LIBs in the 1990s by Sony Company.

However, many issues in SEI still need to be addressed, such as how to *in-situ* characterize the dynamic variation of SEI, and then how to build a scientific relationship between the SEI and the electrode

Cite as: Cheng H R, Ma Z, Guo Y J, Sun C S, Li Q, Ming J. Which factor dominates battery performance: Metal ion solvation structure-derived interfacial behaviors or solid electrolyte interphase layer? *J. Electrochem.*, 2022, 28(11): 2219012.

Received: 2022-10-06, Revised: 2022-10-19. *Corresponding author, Tel: (86-431)85262592, E-mail: jun.ming@ciac.ac.cn

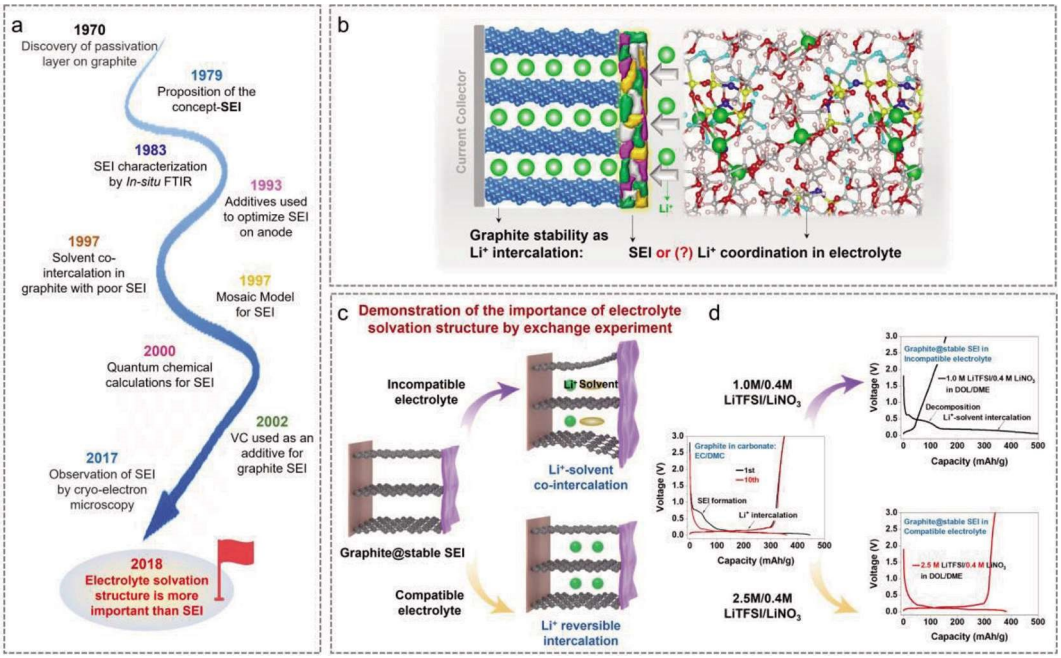

Figure 1 Revisit the role of SEI on graphite electrodes. (a) Development history of SEI formed on the graphite electrode. (b) Controversial influences of the SEI and solvation structure on the graphite electrode performance. (c) Schematic diagram and (d) the varied graphite performance examined by exchange experiment. ((b, d) Reproduced with permission of Ref. 33. Copyright 2018 American Chemical Society.) (color on line)

performance[23-26]. A bunch of advanced techniques have been developed to study the effect of SEI on electrode performance, including X-ray photoelectron spectroscopy (XPS)[27], time-of-flight secondary ion mass spectrometry (TOF-SIMS)[28, 29], and cryo-transmission electron microscopy[30, 31]. These methods can only study the products of electrolyte decomposition, but cannot clarify the specific role of SEI. In particular, the commonly believed effect of SEI is being also challenged, as the metal ion solvation structure has been discovered recently to be critical in influencing the battery performance, while the SEI effect is not dominant, such as for the graphite anode that is used for storing the lithium (Li)[32]. It was found that the SEI-coated graphite anode cannot mitigate the electrolyte decomposition and Li^+-solvent co-insertion (i.e., which may cause graphite exfoliation) if an incompatible electrolyte was used instead of the compatible one[33, 34]. This phenomenon is reasonable because changing the electrolyte composition can also alter the Li^+ solvation structure and the spatial arrangement of cation-solvent-anion complex on the electrode surface. This process can indeed affect the metal ions that are extracted from the cathode and/or intercalated into the anode, influencing the battery performance[35-40]. As a result, more and more researchers have realized the crucial role of metal ion solvation structure and its derived (de-)solvation process for battery performance, by which a relationship was also studied to correlate with the battery performance[32, 41-46]. Nonetheless, the improved performances have been artificially attributed to the specific SEI again, which is believed to be formed by the decomposition of the specific solvation structure[18, 47-52]. In stark contrast, the influences of metal ion solvation and the derived (de-)solvation process become equally important. But these factors are still elusive on a molecular scale, as these molecular behaviors are dynamic, abstract, and non-quantitative, and hard to be correlated with the battery performance[33, 34, 53].

In this review, we will summarize our recent research on metal ion solvation structure and the de-

rived metal ion de-solvation behaviors, by which an interfacial model is presented to interpret the electrode and battery performances. We aim to discuss which factors dominate the battery performance, that is, metal ion solvation structure-derived interfacial behaviors or solid electrolyte interphase (SEI) layer. This issue has become a hot and controversial topic in the battery community. This review is timely, as discerning the influence difference between the interfacial behaviors (i.e., interfacial chemistry) and SEI (i.e., interphasial chemistry) is urgent and significant for understanding the battery performance and guiding the electrolyte design. We hope this review could elucidate the importance of metal ion solvation structure, complementing the knowledge of SEI and also facilitating electrolyte design for metal-ion batteries.

2 Emerged Solvation Structure and Interfacial Model

2.1 Raising Controversial Issue of SEI and Solvation Structure Influences

All the stories in this review begin with the SEI formed on the graphite electrode, thus we summarize the development history of the SEI on the graphite anode in Figure 1a[54-57]. The SEI was reported first time on the graphite electrode in 1970, and the concept of SEI on lithium metal was then proposed in 1979 by E. Peled et al[58]. In 1983, *in-situ* characterizations have been developed to monitor the formation of SEI on the electrode surface, where a rough SEI model was presented[59]. In 1997, the classic "mosaic model" was finally built[60]. During the period of this time, the most successful case of forming SEI on the electrode is the carbon-based anode (e.g., graphite)[61]. For example, a good SEI can be formed on the graphite anode by employing EC-based electrolyte, and then enables a reversible Li^+ (de-)intercalation with the graphite, thereby achieving the final commercialization of the LIBs[22]. In contrast, an inferior SEI could be formed on the graphite anode in the PC-based electrolyte, in which the Li^+ (de-)intercalation cannot be guaranteed[62]. Based on these discoveries, it was concluded that a good SEI is a necessity for a reversible Li^+ (de-)intercalation within graphite, while an inferior SEI may cause the Li^+-solvent co-intercalation (i.e., graphite exfoliation). Afterwards, many researches about the quantum chemical calculations have been carried out to engineering the SEI by electrolyte design since 2000[63]. The introduction of additives such as the vinylene carbonate (VC) additive in 2002 in the electrolyte to form better SEI on graphite anode is another achievement[64], as the formed SEI can enhance Coulombic efficiency and the stability of the electrode significantly. Later, engineering the SEI by designing and adding additives into the electrolyte has become mainstream in the battery community. As a counterpart, the SEI formed on the cathode (i.e., CEI) has been also studied[65]. In addition, a bunch of techniques have been also developed to study the SEI, including the advanced cryo-transmission electron microscopy, by which we can observe the varied morphologies of the SEI[30, 31, 66, 67].

However, the viewpoint of the SEI effect that dominates graphite performance has been questioned in 2008. Ming et al found that the metal ion (i.e., Li^+) solvation structure could dominate the graphite anode performance, that is, reversible Li^+ de-intercalation or Li^+-solvent co-intercalation (Figure 1b)[33]. This new discovery was also proved by an exchange experiment. In detail, a good SEI was pre-formed on the graphite electrode first by several cycles in a compatible electrolyte, such as 1.0 mol·L^{-1} $LiPF_6$ in EC/DMC (1/1, *V*/*V*). Then, such a SEI-coated graphite electrode (i.e., graphite@SEI) was taken out and used to assemble a new battery by employing another kind of electrolyte (Figure 1c-d). It was found that this graphite@SEI cannot sustain the cycle performance when the incompatible electrolyte was used (e.g., 1.0 mol·L^{-1} LiTFSI, 0.4 mol·L^{-1} $LiNO_3$ in DOL/DME, 1/1 in volume ratio), where the electrolyte decompo sition and Li^+-solvent co-intercalation (i.e., graphite exfoliation) occurred immediately (Figure 1c). This result demonstrates that the pre-formed SEI cannot mitigate the Li^+-solvent co-intercalation (i.e., graphite exfoliation) and electrolyte decomposition if the electrolyte is incompatible with the graphite. In stark

contrast, such a graphite@SEI electrode can continually sustain the cycle performance in a new cell when the compatible electrolyte was used (e.g., 2.5 mol·L^{-1} LiTFSI, 0.4 mol·L^{-1} $LiNO_3$ in DOL/DME, 1/1 in volume ratio). In particular, the high Coulombic efficiency of the graphite@SEI electrode in the first cycle demonstrates that the SEI could be well preserved, which can mitigate the electrolyte decomposition effectively (Figure 1d). Thus, herein the issue of SEI that could be damaged and/or dissolved in the exchange experiment can be excluded. The same graphite@SEI electrode was used, but different performances were obtained in different kinds of electrolytes. These results demonstrate that the electrolyte compositions (i.e., Li^+ solvation structure) could also affect the graphite performance significantly, while whether the SEI effect that could be delivered may depend on the electrolyte properties (i.e., compatible, or incompatible).

2.2 Construction of Solvation Structure Model

The question about the SEI effect is further verified by employing the electrolyte with film-forming additives. It is a common belief that the electrolyte additive (e.g., vinylene carbonate (VC), fluoroethylene carbonate (FEC), and vinyl sulfate (DTD), etc.) can participate to form a better SEI, making electrolyte more compatible with the graphite anode (e.g., high Coulombic efficiency, reversible Li^+ (de-)inter calation) (Figure 2a)[68-74]. For example, Ming et al. found that the PC-based electrolyte modified by 6wt% DTD can become compatible with the graphite, enabling a reversible Li^+ (de-)intercalation within graphite. According to the film-forming features of DTD and the common belief of SEI, the formed better SEI should be the main reason for the attained reversible Li^+ (de-)intercalation for the graphite. However, in the exchange experiment, the graphite@SEI cannot sustain the cycle performance when the DTD was removed from the electrolyte[34], implying that the formed SEI cannot mitigate the Li^+-solvent co-intercalation. The conclusion is the same as that in the last part, the SEI effect cannot be delivered well if the electrolyte is incompatible with the graphite. Until 2019, this discovery reminds the researchers to reconsider one question, that is, what the function of additive is, forming a better SEI, changing the Li^+ solvation structure, or both (Figure 2b).

To make this point clearly, Ming et al. presented a solvation structure model to show the varied Li^+ solvation structures in the electrolyte with and without DTD additive. The Li^+ solvation structure model is described by the formula of $Li^+[solvent]_x[additive]_y[anion]$, where the values of x and y can be calculated by the molar contention of the electrolyte. In the electrolyte of 1.0 mol·L^{-1} $LiPF_6$ in PC, the formula of Li^+ solvation structure is $Li^+[PC]_{12.56}[PF_6^-]$, in which 4-5 units of PC molecules coordinate with the Li^+ to form the first layer of the solvation structure while the other PC molecules locate the outer solvation layer (Figure 2c). The anion locates between the first and the outer layers of the solvation structure. In the PC-based electrolyte without DTD additive (i.e., 1.0 mol·L^{-1} $LiPF_6$ in PC, $Li^+[PC]_{12.56}[PF_6^-]$), the strength of Li^+-PC interaction is strong, which leads to the Li^+-PC co-intercalation into the graphite, making the electrolyte incompatible with the graphite (i.e., graphite exfoliation). When the 6wt% DTD was added to the PC-based electrolyte (i.e., 1.0 mol·L^{-1} $LiPF_6$, 6wt% DTD in PC, $Li^+[PC]_{12.56}[DTD]_{0.67}[PF_6^-]$), the DTD can compete with the PC solvent to coordinate with the Li^+ and then dominate the first layer of solvation structure due to its high binding energy (Figure 2d). Then, the Li^+-PC interaction can be weakened significantly, enabling the electrolyte compatible with the graphite (i.e., reversible Li^+ (de-) intercalation). All the conjectures can be confirmed by the varied chemical shift of ^1H NMR and simulation (Figure 2e), where the DTD can dominate the Li^+ solvation structure and weaken the Li^+-PC interaction, thereby mitigating the Li^+-PC co-insertion within the graphite, in turn suppressing the gas production from PC decomposition between graphite layers (Figure 2f).

The model of the Li^+ solvation structure is further demonstrated by using the additives with different

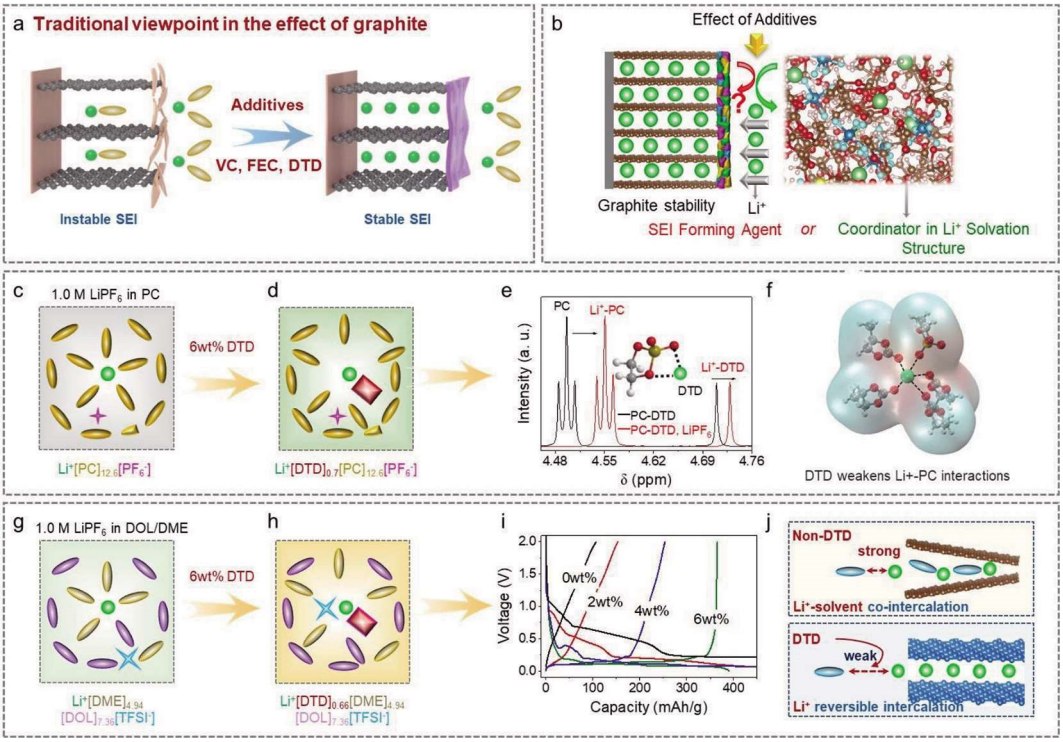

Figure 2 Revisit the role of additive and introduction of solvation structure. (a) Traditional viewpoint of the additives' effect on graphite. (b) Controversial role of additives between the film-forming agent and changing the Li^+ solvation structure to affect the graphite performance. Schematic diagram of the varied Li^+ solvation structure (c) without and (d) with 6wt% DTD in PC-based electrolyte. (e) Comparative NMR spectra and (f) schematic view of the first layer of the Li^+ solvation structure. Schematic diagram of the varied Li^+ solvation structure (g) without and (h) with 6wt% DTD in the ether-based electrolyte. (i) Varied voltage versus capacity profiles of the graphite by using different amounts of DTD additives. ((b-i) Reproduced with permission of Ref. 34. Copyright 2018 American Chemical Society.) (j) Schematic mechanism of additives on affecting graphite performance. (color on line)

coordination capabilities. It was found that the additive with weak coordination capability (e.g., EC, VC) can also change the Li^+ solvation structure, but it is insufficient to make the PC and ether-based electrolytes compatible with graphite. This is because the additives with weak coordination capability cannot weaken the Li^+-solvent interaction effectively, despite some of them (e.g., VC) having a good capability to form SEI. This viewpoint can be further identified in ether-based electrolytes with or without DTD additives. It was found that the DTD additive can also weaken the Li^+-solvent interaction and then make the electrolyte compatible with the graphite in DOL/DME-based electrolyte (Figure 2g-h). In addition, the amount of DTD additive and the coordination capability of additives are demonstrated to be crucial, as these factors determine the changed degree of the Li^+ solvation structure (i.e., Li^+-solvent interaction), then affecting the graphite performance (Figure 2i). Thus, it was concluded that a strong Li^+-solvent interaction may cause a Li^+-solvent co-insertion, while a weak Li^+-solvent interaction is helpful for achieving a reversible Li^+ (de-)interaction (Figure 2j). This is the reason why we observe different graphite performances when the electrolyte compositions are changed, as discussed before.

In this section, besides the proposed Li^+ solvation structure, at least two functions of additives could be found: one is the film-forming effect, the other one is changing the Li^+ solvation structure. Both of them can influence the electrolyte properties and electrode performance, where the amount and the coordination capability of additives can affect and then determine their specific roles. For example, a strong coordination

capability of additives is a precondition that enables the additives coordinate with the Li^+ and then to be reacted to form the SEI layer on the electrode surface. In this way, such kind of additive can be consumed first in the initial cycles to form the SEI to stabilize the electrode, while the residual additive (i.e., supposing the amount of additive is sufficient) can be kept in the electrolyte to change the Li^+ solvation structure (i.e., Li^+-solvent interaction) continually. This is the reason why a very small amount of additives can also change the battery performance, even these additives could be depleted in the initial cycles and disappear in the following cycles. In stark contrast, suppose that the additive has a weak coordination capability, it means that such additive cannot coordinate with the Li^+ and then is hard to be polarized by the Li^+ on the electrode surface to be reacted to form the SEI. In this latter case, such kind of additive can also change the Li^+ solvation structure, but the coordination capability is too weak to weaken the Li^+-solvent interaction sufficiently, as discussed above. Briefly, different amounts and kinds of additives may have different functions in the different electrolytes. Thus, it is challenging to reconsider the roles of additive and SEI in influencing battery performances, at least for the most commonly used graphite anode.

2.3 Construction of Solvation Structure Derived Interfacial Model

The SEI effect can neither interpret the varied graphite performance in different ester- or ether-based electrolytes[75, 76]. Although the presented factor of the Li^+-solvent interaction in the Li^+ solva tion structure can interpret whether the electrolyte is compatible with the graphite or not, it is insufficient to interpret the varied capacity and electrolyte stability in Figure 3a-d. For example, when 1.0 mol·L^{-1} $LiPF_6$ was used, why the linear DEC-based electrolyte is incompatible with graphite, while the other linear ester-based electrolyte (e.g., DMC, or EMC) is compatible (Figure 3a). Besides, why a large polarization exists in the voltage versus capacity profile when the EC is used as the single solvent in the electrolyte? In addition, the EC and DEC electrolytes are both incompatible with the graphite, why EC/DEC-based electrolyte becomes compatible (Figure 3b). Moreover, why the cyclic ester solvent with different substituents has different compatibility with graphite electrodes, and also why most ether-based electrolytes are incompatible with graphite (Figure 3c-d). These phenomena are difficult to be explained neither from the influences of different SEI layers nor from the Li^+-solvent interaction only. We have to figure out the difference from the interfacial chemistry and then correlate it to the graphite electrode performance (Figure 3e).

Ming et al. have constructed an interfacial model in 2019 based on the Li^+ de-solvation process, which can correlate to the graphite performance (Figure 3f).[53] Based on the interface model, the parameters of *L* and *B* are presented (Figure 3g). The *L* represents the conformation and strength of the Li^+-solvent interaction, these properties are related to the dielectric constant of the solvent and the coordination ability with the Li^+. While the *B* represents the solvent steric interactions between the molecules, these properties are related to the size of solvent molecules and intermolecular interaction. For example, the *L* value of EC molecules is high and the *B* value is low, demonstrating the high binding energy of the Li^+-EC pair and also a tight stacking form of EC molecules on the electrode surface. In addition, the Li^+-solvent-anion complex in the interfacial model is also presented, as its properties can correlate to the kinetic, thermodynamic, and electrochemical stabilities of electrolytes (Figure 3g). Then, Ming et al. further summarize the relationship between the *L*, *B* values and the graphite performance in different single solvent-based electrolytes. It was found that a compatible (i.e., the yellow regions) and an incompatible region (i.e., the blank regions) can be divided in the coordinate system (Figure 3h). In this way, the compatibility of the electrolyte can be tuned readily by tuning the *L* and *B* values in the interfacial model. These values can be tuned by varying the kinds of solvent, types of metal salts, and electrolyte concentrations. And also, the varied graphite performance can be interpreted based

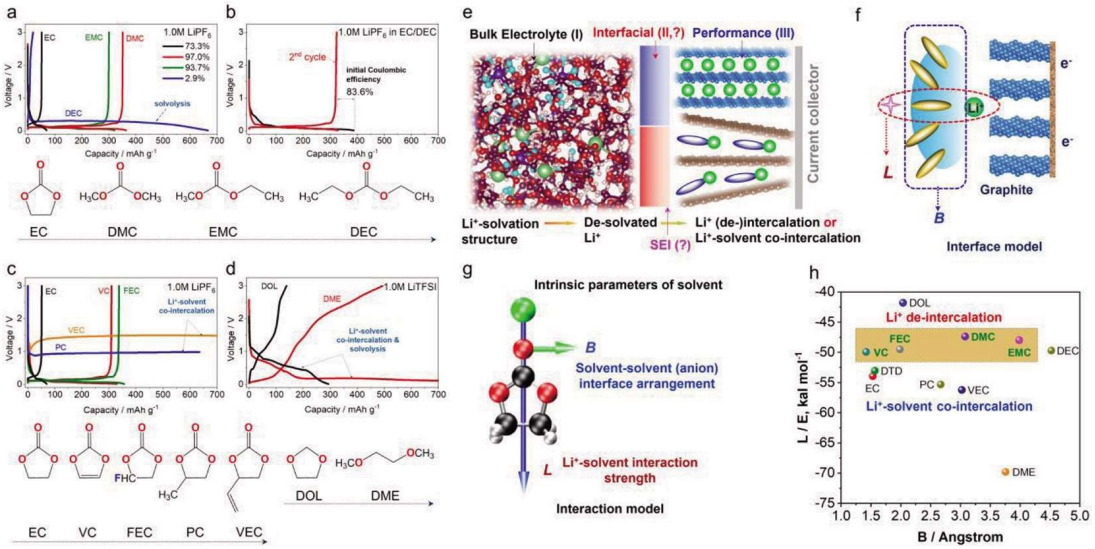

Figure 3 Molecular interfacial model on graphite electrode. (a-d) Unexplained graphite performances in different electrolytes. (e) Correlation between interfacial chemistry and graphite performance needs to be explored. (f) Constructed interfacial model and (g) typical meaning of the parameters of *L* and *B* using EC molecule as an example. (h) Correlation between the *L* and *B* values in the interfacial model and graphite performance. ((a-h) Reproduced with permission of Ref. 53. Copyright 2019 American Chemical Society.) (color on line)

on the interfacial model, which seems more reasonable than the SEI-based interpretation.

For example, in an EC-based electrolyte, a strong, symmetric interaction of Li^+-EC (i.e., *L*) and the tightest stacking form of EC-EC (i.e., *B*) exists in the interfacial model, which makes the Li^+ difficult to be de-solvated, leading to a large polarization. In a DEC-based electrolyte, the DEC solvent that coordinates with the Li^+ has a low electrochemical stability, resulting in the easy decomposition of DEC on the graphite electrode surface. In stark contrast, when the EC/DEC mixed solvent is used in the electrolyte, the Li^+-EC pair can dominate the interfacial model due to its higher binding energy compared to that of Li^+-DEC. Then, the DEC can arrange behind the EC, which not only can weaken the Li-EC interaction to facilitate the Li^+ de-solvation and (de-)intercalation, but also can enhance its electrochemical stability, as the DEC can keep far from the electrode surface to avoid the polarization by the Li^+ (Figure 4a). In addition, the electrolyte additive can also change the *L* and *B* values in the interfacial model by changing the Li^+ solvation structure (Figure 4b). For example, in the PC or VEC-based electrolytes, the strong and asymmetric interaction of Li^+-PC or Li^+-VEC (i.e., high *L* value) in the interfacial model can be weakened by the DTD additives, making the electrolyte become compatible (i.e., a reversible Li^+ (de-)intercalation) (Figure 4b). Herein one may consider how 6wt% DTD can tune the *L* value of Li^+-PC in PC-based electrolytes, moving to the yellow region when the *L* values of Li^+-DTD and Li^+-PC are both below the yellow region in Figure 2h. This should be ascribed to the interaction between PC and DTD in the interfacial model (i.e., the value of *B*) as it can also affect the Li^+-solvent interaction. Moreover, the excellent compatibility of the high-concentrated electrolyte can be also explained by the interfacial model. Taking the DME-based electrolyte as an example (Figure 4c), the DME solvent is prone to be co-inserted with the Li^+ into the graphite due to its strong and symmetric Li^+-DME interaction (i.e., high *L* value). This issue can be addressed by increasing the Li salt concentration (e.g., LiTFSI), as the Li^+-DME interaction can be weakened by the $TFSI^-$ when the amount of $TFSI^-$ is increased to a certain value (Figure 4c)[53]. This expla-

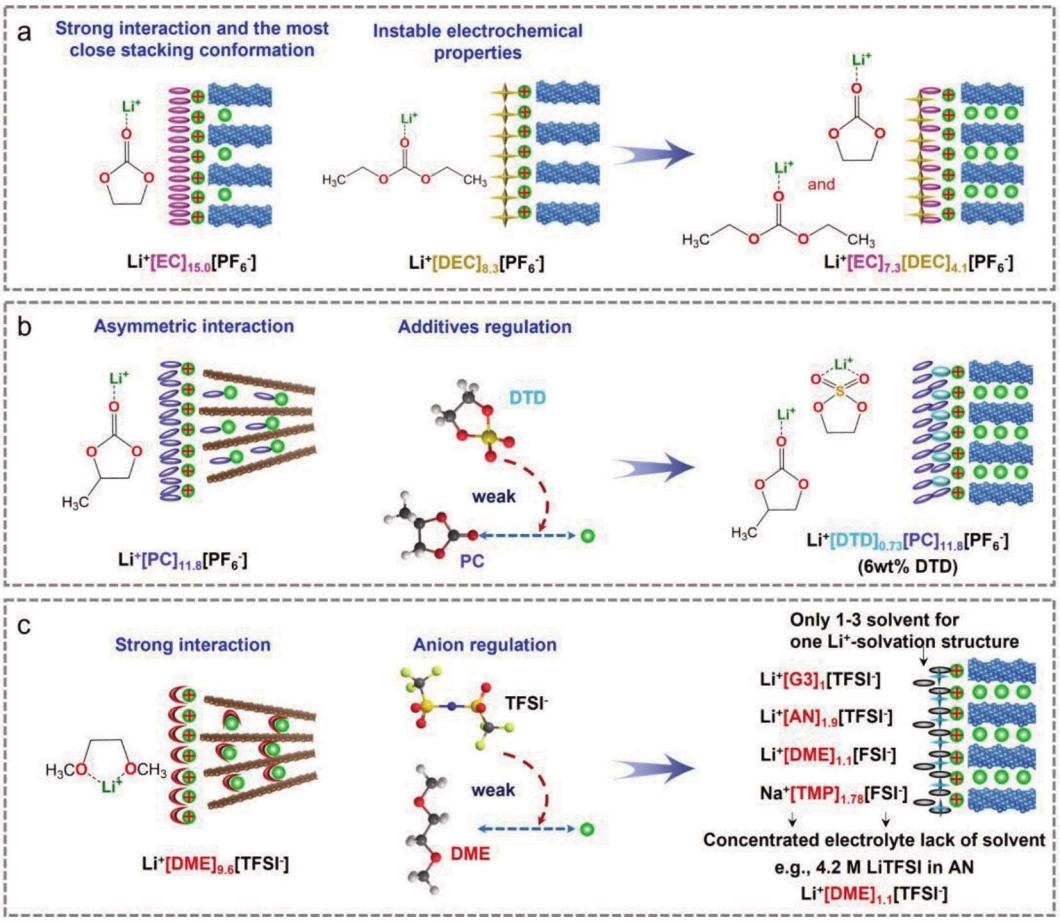

Figure 4 Interface model interpreting the varied graphite performance. Cases of regulating the L and B values in the interfacial model by varying the kinds of (a) solvent, (b) additive, and (c) concentration. ((a-c) Reproduced with permission of Ref. 53. Copyright 2019 American Chemical Society.) (color on line)

nation can be further applied to other kinds of concentrated electrolytes, where only a 1-3-unit solvent was used in most cases[38, 47, 77]. In this way, the solvent is insufficient, the anions can weaken the Li^+-solvent interaction effectively in the interfacial model and then enable a reversible Li^+ (de-)intercalation (Figure 4c). In brief, according to the interfacial model, we can interpret the electrolyte compatibility and graphite performance readily, and the influences of SEI on electrolyte compatibility and graphite performance readily, where the influences of SEI are found to be not dominant.

2.4 Interface Model on Graphite Electrode in Potassium Ion Battery

The universality of the as-proposed interfacial model can be further verified by the graphite anode in potassium ion batteries (KIBs). Two competing reaction paths of K^+-solvent-anion complex are presented, as these reaction paths can be expected on the graphite surface: one is the de-solvation of K^+ on the graphite surface, where the K^+ can be de-solvated readily and intercalated into the graphite, indicating the compatibility of electrolyte; the other one is the K^+-solvent co-insertion within the graphite, indicating the incompatibility of electrolyte with the graphite (Figure 5a)[78]. The latter case is always caused by the strong K^+-solvent interaction (i.e., high L value), by which the K^+-solvent could be co-inserted into the graphite and/or K^+-solvent-anion complex could be decomposed, resulting in the graphite exfoliation and/or electrolyte decomposition on the graphite surface. In this way, by varying the concentration of

potassium salt and/or the type of solvent, we could tune the properties of K^+-solvent-anion (e.g., the value of L) and the conformation of solvent-solvent stacking form (i.e., B), achieving a de-solvation of the K^+, in turn making the electrolyte compatible with the graphite. This conjecture is confirmed in the PC-based electrolyte. We found that the PC-based electrolyte is incompatible with the graphite when the KFSI concentration was lower than 3.0 mol·L^{-1}, where the K^+-PC co-intercalation, graphite exfoliation, and electrolyte decomposition can be induced due to the strong K^+-PC interaction (Figure 5b). In stark contrast, when the KFSI concentration increased to 3.0 mol·L^{-1} (i.e., $K^+[EMC]_{2.4}[FSI^-]$), the FSI^- anion could appear around the K^+ on the graphite electrode surface, which can decrease the polarization of K^+-solvent and also weaken the K^+-PC interaction, thereby facilitating the K^+ de-solvation and (de) intercalation within the graphite, inhibiting the co-intercalation of K^+-PC (Figure 5b-d). In this way, when a different solvent is used in the electrolyte, the L and B values can be tuned readily by the concentration of potassium salt, achieving an appropriate interfacial model for a reversible K^+ (de-) intercalation within the graphite (Figure 5e).

The interfacial model can be further tuned by adding additives with strong coordination capacity, such as the DTD. Ming et al. found that 6wt% DTD can make the electrolyte of 1.0 mol·L^{-1} KFSI in trimethyl phosphate (TMP) compatible with the graphite anode, without the need of employing the concentrated electrolyte strategies (Figure 5f-g)[79]. This is reasonable, as the DTD can regulate the solvation structure of K^+ from $K^+[TMP]_{8.7}[FSI^-]$ to $K^+[TMP]_{8.7}$

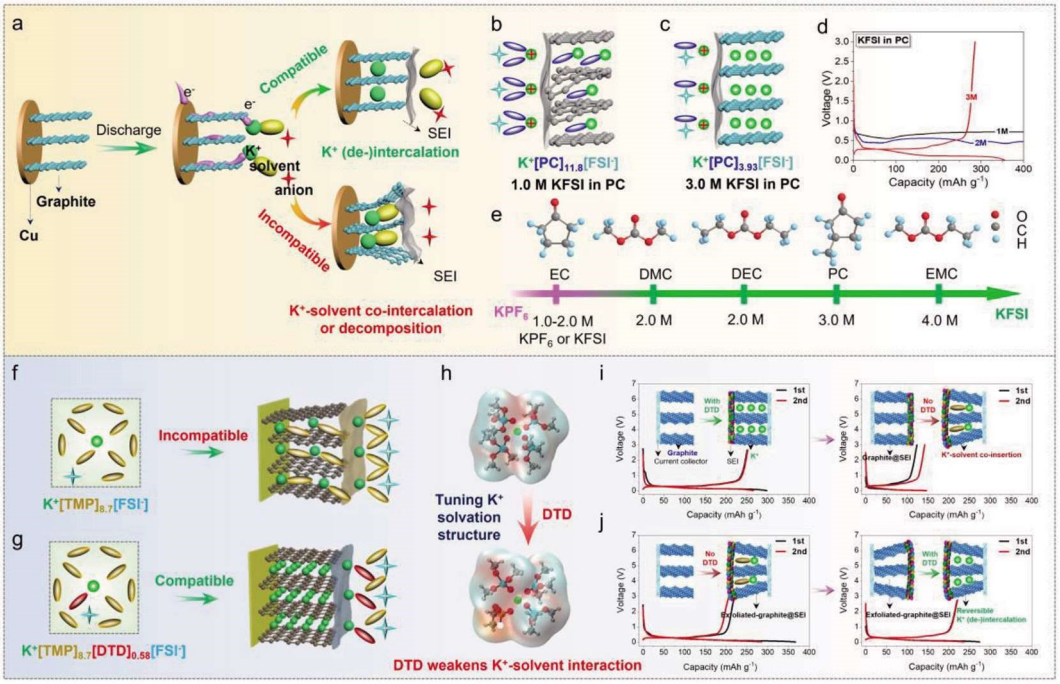

Figure 5 Designing electrolytes compatible with graphite electrode in KIBs. (a) Competitive reaction pathways for K^+-solvent structure on the graphite surface. Interfacial model of (b) 1.0 mol·L^{-1} and (c) 3.0 mol·L^{-1} KFSI in PC-based electrolyte. (d) Varied graphite performance in PC-based electrolyte by using different concentrations. (e) Requested potassium salt concentrations for the different solvents to make the electrolyte compatible with the graphite. ((a-e) Reproduced with permission of Ref. 78. Copyright 2020 American Chemical Society.) Varied K^+ solvation structure and interfacial model (f) without and (g) with DTD additives in TMP-based electrolyte. (h) Comparative snapshot of the first layer of the K^+ solvation structure without and with DTD additives. Exchange experiment of the graphite electrode (i) from compatible to incompatible electrolyte and (j) from incompatible to compatible electrolyte. ((f-j) Reproduced with permission of Ref. 79. Copyright 2020 Wiley-VCH.) (color on line)

$[DTD]_{0.58}[FSI^-]$, in which the DTD can weaken the K^+-TMP interaction significantly (i.e., low *L* value) (Figure 5h). Thus, K^+ can be de-solvated from the interfacial model and (de-) intercalated within the graphite reversibly. Herein, we would like to note that the reason why increasing the KFSI concentration in TMP electrolyte can make the electrolyte compatible with the graphite is also the weakened K^+-PC interaction[78], which is the same as that adding DTD additive. One may consider that the variation may come from influences of SEI. Ming et al. employed the same exchange experiment to confirm that the root cause comes from the difference in the K^+ solvation structure and interfacial model. It was found that the graphite@SEI (i.e., pre-formed in the TMP-based electrolyte with DTD) cannot sustain the cycling performance when it was reassembled in a new battery using the TMP-based electrolyte without DTD (Figure 5i). In stark contrast, the exfoliated-graphite @SEI (i.e., pre-cycled in TMP-based electrolyte without DTD) electrode could re-attain a high capacity of 225 $mAh \cdot g^{-1}$ by employing the TMP-based electrolyte with DTD (Figure 5j). The comparative results demonstrate that the strength of K^+-TMP interaction determines the electrolyte compatibility with the graphite, rather than the SEI formed on the graphite electrode. In this section, the importance of the metal ion solvation structure and the derived interfacial model is further confirmed by employing the graphite anode in KIBs, while the effect of the formed SEI is not a dominant factor to affect the graphite performance.

3 Interfacial Model on Lithium Metal Electrode in Lithium Batteries

The proposed interfacial model can be also affected by the electrode properties, which is feasible to apply in lithium metal batteries to interpret the varied lithium plating/stripping behaviors[80]. For example, in the typical ether-based electrolyte of 1.0 $mol \cdot L^{-1}$ LiTFSI, 0.4 $mol \cdot L^{-1}$ $LiNO_3$ in DOL/DME (i.e., $Li^+[DME]_{4.83}[DOL]_{7.19}[TFSI^-]_{0.91}[NO_3^-]_{0.09}$) (Figure 6a), Ming et al. reported that the Li could be plated uniformly on the 3D Cu_2O and Cu nanorod arrays (3D Cu_2O/Cu) electrode with a high Coulombic efficiency of 98.6%, while a serious electrolyte decomposition and lithium dendrite growth were obtained on the 3D Cu/Cu electrode. The different phenomenon can be elucidated by the different interfacial models relating to the electrode property effect, rather than the spatial structure effect. In detail, in the discharge process, a layer of Li_2O can be formed on the electrode by the reaction between the Li and 3D Cu_2O/Cu electrode, facilitating to form a stable interfacial model and also reducing the electron-donating capability of the electrode (Figure 6b). In contrast, on the 3D Cu/Cu electrode, the formed interfacial model (layer) is not stable, and also the electron-donating and catalytic capability of Cu is high, leading to a serious electrolyte decomposition and Li dendrite growth (Figure 6c). Note that this is the first time to show that the electrode properties can affect the validity of interfacial model, that is the arrangement of Li^+-solvent-anion complex, which can determine the electrolyte stability and electrode performance.

Ming's interfacial model can also interpret the different Li plating phenomena when the solvent was changed in the electrolyte[81]. For example, in the electrolyte of 1.0 $mol \cdot L^{-1}$ $LiPF_6$ in EC (i.e., $Li^+[EC]_{15.56}[PF_6^-]$), the Li is hard to be plated on the Cu foil due to the strong interaction of Li^+-EC and the tight stacking form of EC molecules (i.e., low B value) in the interfacial model (Figure 6d). In the electrolyte of 1.0 $mol \cdot L^{-1}$ $LiPF_6$ in EMC (i.e., $Li^+[EMC]_{9.73}[PF_6^-]$), the electrolyte was severely decomposed due to the low electrochemical stability of Li^+-EMC cluster (Figure 6e). In stark contrast, in the electrolyte of 1.0 $mol \cdot L^{-1}$ $LiPF_6$ in EC/EMC (i.e., $Li^+[EC]_{7.78}[EMC]_{4.87}[PF_6^-]$), the EC can occupy the electrode surface due to the stronger Li^+-EC interaction than the Li^+-EMC, and then the EMC tends to be distributed behind the EC molecules. In this way, the Li^+-EC interaction can be weakened by EMC, making Li^+ de-solvate easily and deposit on the electrode (Figure 6f). Meanwhile, the polarization of the EMC induced by the Li^+ can be also mitigated by the EC in the interfacial model, then the EMC shows the improved electrochemical stability.

Finally, a uniform Li plating/stripping can be observed in the EC/EMC-based electrolyte. This explanation is similar to the previous one why EC/DEC-based electrolytes are compatible with graphite electrodes while EC or DEC-based electrolytes are incompatible.

Based on the interfacial model, it is easy to understand why a low Coulombic efficiency (CE) (i.e., less than 20%) is always obtained in Li||Cu asymmetric cell when a single DMC, EMC or DEC solvent was used in the electrolyte. This is because the electrochemical stabilities of DMC, EMC or DEC solvent in the interfacial model can be reduced significantly when the solvent is induced by the Li^+, then leading to a severe electrolyte decomposition. When the EC molecule is used as a single solvent in an electrolyte, a unstable CE value fluctuates in a wide range, as the Li^+-EC interaction becomes too strong in the interfacial model to be deposited uniformly (Figure 6g). In stark contrast, when the EC is added as a co-solvent into the single linear ester-based electrolyte, the CE value could become stable and also increased to more

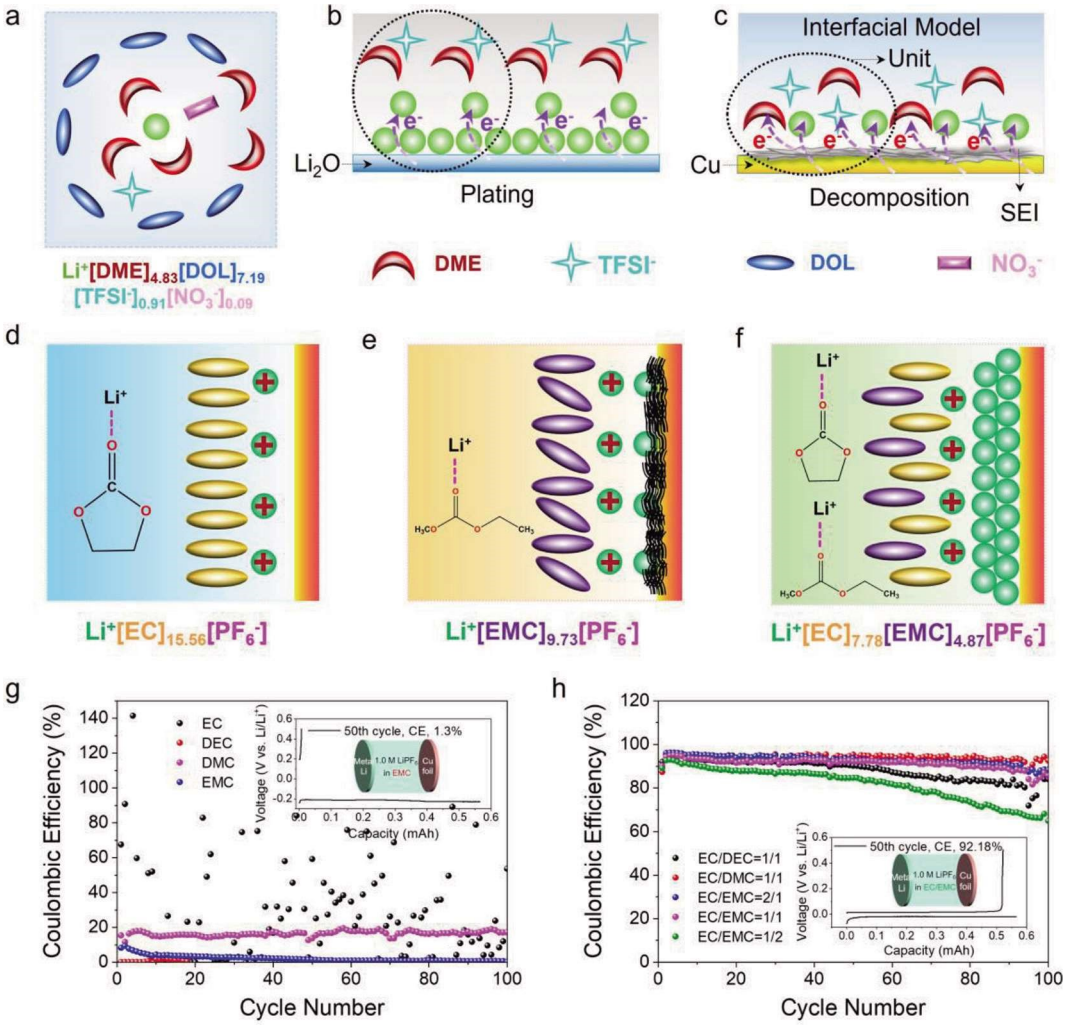

Figure 6 Interfacial model interpreting the varied lithium plating/stripping performances. (a) Schematic Li^+ solvation structure of the $Li^+[DME]_{4.83}[DOL]_{7.19}[TFSI^-]_{0.91}[NO_3^-]_{0.09}$. Comparative interfacial models on (b) 3D Cu_2O/Cu and (c) 3D Cu/Cu current collector surface. ((a-c) Reproduced with permission of Ref. 80. Copyright 2021 American Chemical Society.) (d-f) Interfacial model of $Li^+[EC]_{15.56}[PF_6^-]$, $Li^+[EMC]_{9.73}[PF_6^-]$ and $Li^+[EC]_{7.78}[EMC]_{4.87}[PF_6^-]$ on Cu current collector surface. Comparative Coulombic efficiency of the Li || Cu asymmetric cell in the electrolytes of using (g) single solvent and (h) mixed solvents with the EC. ((d-h) Reproduced with permission of Ref. 81. Copyright 2021 American Chemical Society.)(color on line)

than 90% (Figure 6h). The improved performance is ascribed by the specific interfacial model, which is similar to that in Figure 6f. The linear ester-based solvent can weaken the Li^+-EC interaction, while the EC can improve the electrochemical stability of linear ester-based solvent by its separation effect (Figure 6h). All these results show the feasibility of the interfacial model to interpret the performance in Li metal batteries, which differs from the SEI-based interpretation. In this study, Ming et al. also in the first time showed the new effect of EC which can stabilize the electrolyte by dominating the interfacial model[81]. This result also demonstrates that we have to be very prudent when we design the EC-free high voltage electrolyte, as it may be less compatible with the graphite anode from the EC-free interfacial model. In other words, we have to tune the electrolyte composition in a good manner to get a stable and fit in the EC-free interfacial model, otherwise, a severe electrolyte decomposition could be observed at the anode side.

4 Interfacial Model on Sodium or Potassium Metal Electrode in Metal Batteries

The same progress has been made in sodium/potassium metal battery, where the proposed solvation structure and interfacial model are also helpful to address the issues of electrolyte incompatibility with sodium or potassium metal electrodes. Ming et al. have presented that two competing reaction pathways can occur on the metal electrode during the Na^+ or K^+ de-solvation[82]. which is similar to those occurred on the graphite surface in lithium or potassium ion batteries (Figure 5a)[78]. In the first pathway, when the M^+-solvent-anion ($M^+ = Na^+, K^+$) is thermodynamically stable, the M^+ can be de-solvated from the M^+-solvent-anion complex and then plated on the electrode after accepting one electron. This process means that the electrolyte is compatible with the electrode, enabling stable cycling of the battery. In contrast, when the M^+-solvent cluster is thermodynamically unstable, the electrons can be transferred from M^+ to the solvent-anion cluster, leading to a continuous decomposition of electrolyte (Figure 7a). This latter pathway means that the electrolyte is incompatible.

Ming et al. also indicated that the priority of the two pathways is determined by the molecular orbital energy levels of M^+-solvent-anion in the interfacial model. The parameter of ΔE, that is the energy difference between the highest occupied molecular orbital' (HOMO') and the lowest unoccupied molecular orbital (LUMO), is proposed to evaluate the stability of the M^+-solvent-anion cluster. Herein, the LUMO is used to represent the frontier orbital of the K^+-solvent-anion cluster, which becomes HOMO' (i.e., K^0-solvent-anion) after gaining an extra electron. The higher ΔE is, the more stable is the electrolyte, as the large orbital difference leads to difficulty in electron transfer from M^+ to solvent-anion cluster (Figure 7b). According to these analyses and parameters, Ming et al. showed that the concentrated DME-based electrolyte employing KFSI salt (e.g., 5.0 mol·L^{-1} KFSI in DME) demonstrated a low polarization and high CE in potassium metal battery compared to the electrolyte using ester-based solvent or KPF_6 salt (Figure 7b)[82].

Ming et al. also introduced a sodium solvation structure and an anion-based interfacial model in sodium metal battery to interpret the varied sodium plating/stripping behaviors in different electrolytes (Figure 7c), where the feasibility of the ΔE was also further confirmed (Figure 7d).[83] It was found that the ClO_4^- and $CF_3SO_3^-$ can stay close to the sodium metal anode due to the low steric hindrance of ClO_4^- (i.e., low B value) or the strong interaction between $CF_3SO_3^-$ and Na^+ (i.e., high L value) (Figure 7e). In addition, the ΔE value of Na^+-solvent-ClO_4^- and Na^+-solvent-$CF_3SO_3^-$ is also much lower than that of Na^+-solvent-PF_6^-, thus showing a severe electrolyte decomposition, low CE and inferior cycling performance (Figure 7f). In contrast, the PF_6^- can locate sightly far from the sodium metal interface in DME-based electrolytes (i.e., $Na^+[DME]_{9.61}[PF_6^-]$) due to the moderate L and B in the interfacial model, where the ΔE value of Na^+-solvent-PF_6^- is also high,

thus showing a good electrolyte stability, high CE and long cycling performance (Figure 7g). In this section, besides the L and B values, the thermodynamical and electrochemical properties of M^+-solvent-anion are discussed, which can complement the knowledge in the interfacial model. This analysis is also feasible for the lithium metal batteries in the last section. Based on the interfacial model, a different view angle has been proposed for the design of metal compatible electrolyte, in which the importance of M^+-solvent-anion is emphasized that needs to be precisely regulated to achieve a good compatibility, high Coulombic efficiency, and low polarization in metal batteries. This viewpoint differs from the SEI-based interpretation, which can be verified by the exchange experiment.

5 Interfacial Model on Alloying Anode in Metal Ion Batteries

Ming et al. further applied the proposed interfacial model to design the electrolyte for stabilizing the alloying anode (e.g., Sn, Sb, Bi, Si, etc.), aiming to mitigate the capacity decay and the battery failure. During the cation de-solvation process, two competitive reaction pathways can be also expected for the M^+-solvent-anion complex on the alloying anode surface (Figure 8a)[84]. When the M^+-solvent-anion complex is thermodynamically stable after accepting one electron, the M^+ could be de-solvated to proceed with the alloying process, under which the electrolyte is considered to be compatible with the alloying electrode. In contrast, when the M^+-solvent-anion complex is thermodynamically unstable after accepting one electron, the M^+-solvent-anion complex could be decomposed, under which the electrolyte is considered to be incompatible with the alloying electrode. In the latter case, the capacity of the alloying anode will decay fast, and the battery will be expired soon, as the SEI would accumulate continually on the alloying anode by electrolyte decomposition accompanying the pulverization of the electrode until the depletion of electrolyte and the final expiry of battery. According to the proposed interfacial model, a compatible electrolyte with the requested sodium solvation structure and interfacial model were designed by tuning the kinds of solvent and metal salt. In the electrolyte of 1.0 mol·L^{-1} $NaPF_6$ in DME (i.e., $Na^+[DME]_{9.6}[PF_6^-]$), the capacity of the micro-sized Sn alloying anode can be well stabilized (Figure 8), where a high capacity of over 650 mAh·g^{-1} and high-capacity retention of 85.3% after 200 cycles could be obtained (Figure 8b-c)[85]. In contrast, in the DME-based electrolyte, the capacity of such Sn alloying anode could not be stabilized when the PF_6^- anion was changed to $CF_3SO_3^-$ or ClO_4^- (Figure 8d-e), demonstrating the incompatibility of the electrolyte. This result is consistent with the high ΔE value of Na^+-DME-PF_6^-, which means that the electrolyte has good thermodynamic and electrochemical stabilities (Figure 7d).

Ming et al. also designed a compatible electrolyte for the alloying anode in the potassium ion battery. It was found that the Sb alloying anode became well stabilized in 4.0 mol·L^{-1} KFSI in DME-based electrolyte (i.e., $K^+[DME]_{2.4}[FSI^-]$) (Figure 8f), achieving a high capacity of 628 mAh·g^{-1} and stable cycling performance more than 100 cycles (Figure 8g). In contrast, when the other kind of solvent (e.g., EC/EMC), potassium salt (e.g., KTFSI), or dilute concentration (e.g., 2.0 mol·L^{-1} KFSI) was used, the Sb alloying anode could not be stabilized (Figure 8g). The good electrolyte compatibility of the as-designed electrolyte should be ascribed to the high ΔE value of K^+-DME-FSI^-, implying high thermodynamic and electrochemical stabilities. One may still question that the varied electrode performance may come from different effects of the formed SEI in different electrolytes. Ming et al. excluded this possibility by the exchange experiment, by which the importance of the interfacial model was further verified[84]. For example, the bulk Sb electrode was assembled in a half cell using the compatible electrolyte (e.g., 4.0 mol·L^{-1} KFSI in DME) and then cycled for 9 cycles to form an SEI-coated Sb electrode (i.e., Sb@SEI). Then, such a Sb@SEI electrode was used to reassemble a new battery by employing an incompatible electrolyte (e.g., 0.8 mol·L^{-1} KPF_6 in EC/DEC) (Figure 8h). It was found that the Sb@SEI electrode expired fast after 20

cycles (Figure 8i). In contrast, the pre-formed Sb@SEI electrode that almost expired in the incompatible electrolyte (e.g., 0.8 mol·L^{-1} KPF_6 in EC/DEC) could demonstrate a high capacity and good cycling performance once a compatible electrolyte (i.e., 4.0 mol·L^{-1} KFSI in DME) was used (Figure 8j-k), even though the electrode was slightly pulverized. These results confirm that the formed SEI cannot stabilize the alloying anode if the electrolyte is incompatible, which means that the properties of the M^+-solvent-anion complex in the interfacial model is the dominant factor to determine the electrode performance.

This viewpoint has recently been further confirmed in lithium-ion batteries, where a series of compatible ether-based electrolytes, such as 1.2 mol·L^{-1} LiFSI in triethyl phosphate/1,1,2,2-tetrafluoroethyl-2,2,3,3-tetrafluoropropyl ether (TEP/HFE, 1/3 in molar/molar ratio)[86], 3.75 mol·L^{-1} LiFSI/0.5 mol·L^{-1} lithium difluoro (oxalato) borate (LiDFOB) in DME[87], 1.5 mol·L^{-1} LiFSI/0.2 mol·L^{-1} LiDFOB additive in DME/HFE (4/6 in volume ratio) [88], were designed by Ming et al. to stabilize the antimony (Sb) anode. This breakthrough is hard to be achieved before engineering the SEI, as the alloying anode is hard to be stabilized in storing lithium. Particularly, Ming et al. demonstrated that the SEI can reduce the direct contact between the electrode and electrolyte, and then mitigate the electrode's electron-donating capability to Li^+-solvent-anion complex, which in turn increase the electrolyte stability (e.g., electrochemical stability of Li^+-

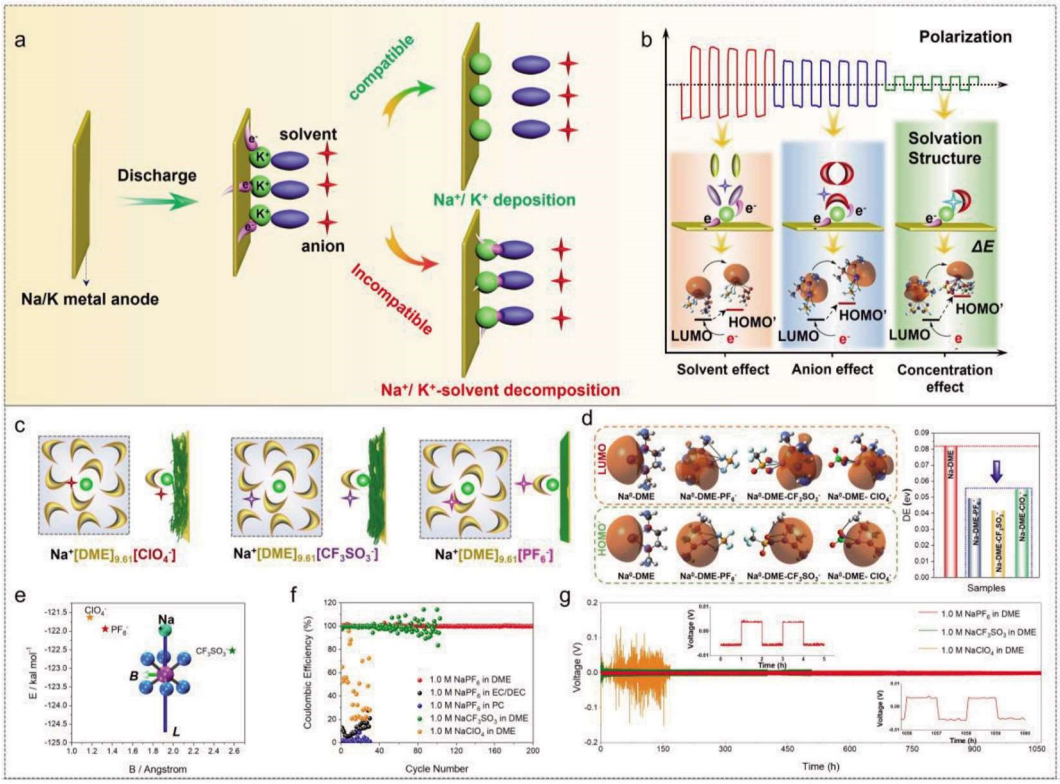

Figure 7 Designing electrolytes compatible with potassium and sodium metal anodes. (a) Two competing reaction pathways of K^+-solvent-anion complex on the K metal anode surface. (b) Varied ΔE, interfacial model, and plating/stripping performance tuned by the solvent, anion, and concentration. ((a, b) Reproduced with permission of Ref. 82. Copyright 2020 American Chemical Society.) (c) Solvation structure and interfacial model of Na^+ in DME-based electrolyte with different anions. (d) Comparative LUMO, HOMO′, and ΔE of the Na^+ solvation structure. (e) Simulated Na^+-anion binding energy (L) and the half distance between the adjacent anion (B). (f) Comparative Coulombic efficiency of the Na || Cu asymmetric cell and (g) the voltage-time curves of Na || Na symmetrical cells using different kinds of electrolyte. ((c-g) Reproduced with permission of Ref. 83. Copyright 2020 American Chemical Society.) (color on line)

solvent-anion). This is the first time to discern the roles of the interfacial behavior and SEI layer for stabilizing the electrode in lithium-ion batteries by employing the Sb alloying anode as an example[87,88].

6 Construction of Cathode and Anode Interfacial Models in Full Batteries

The importance of the interfacial model is emphasized on the anode in the above sections, during this period rare attention has been paid to the interfacial model on the cathode side. This is because the cathode electrolyte interphase (CEI) formed on the cathode has been regarded as the dominant factor to stabilize the cathode since 2004, by which the electrolyte oxidation and the corrosion of cathode materials can be mitigated, especially under high-voltage operation[65, 89-92]. Moreover, it is hard to apply the molecular behaviors in the anode interfacial model to the cathode indiscriminately, as the cation (de-)solvation behaviors at the cathode and anode interfaces are different, let alone discerning their influences from the CEI.

Until 2021, Ming et al. presented a cathode interface model and constructed the dynamic mutual-interaction interfacial behavior on the cathode and anode simultaneously in graphite || NCM622 battery (Figure 9a)[93]. This model shows the interaction of

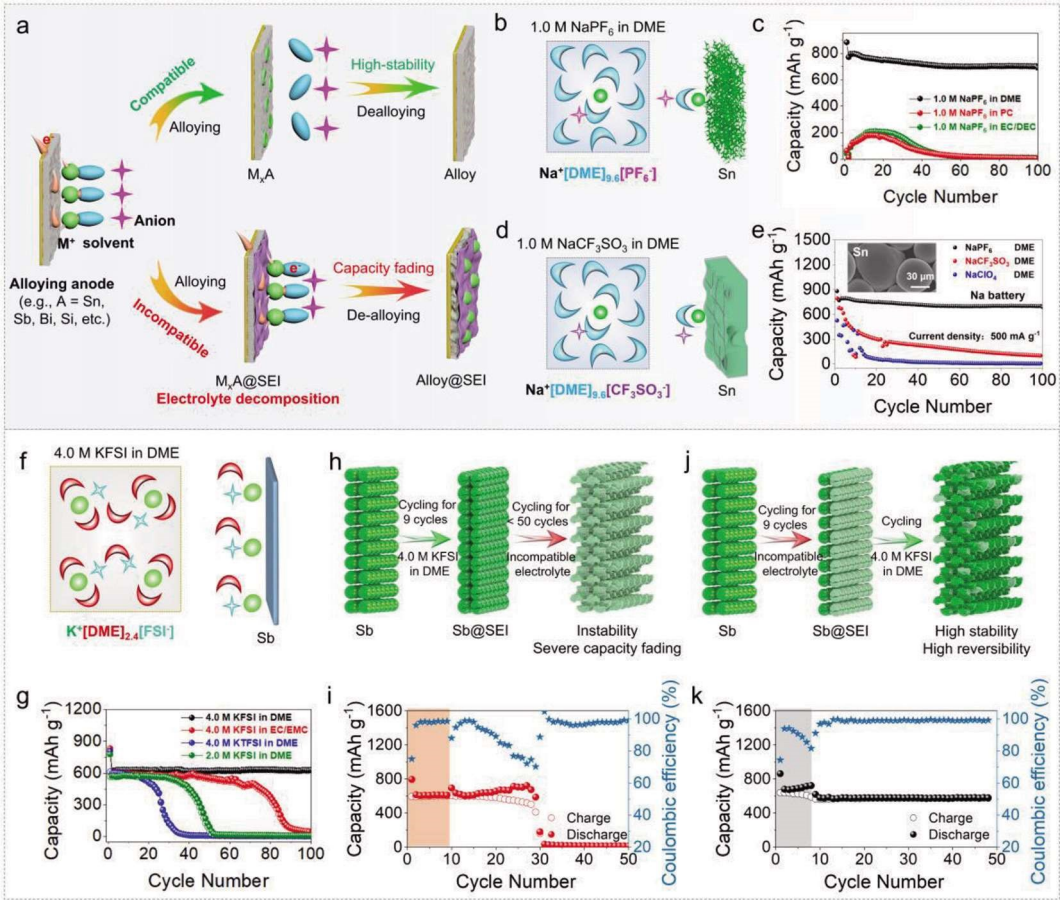

Figure 8 Designing electrolytes compatible with alloying anodes. (a) Two competitive reaction pathways for M^+-solvent-anion complex on the alloying anode. (b) Na^+ solvation structure and interfacial model on the bulk Sn anode in the electrolyte of $Na^+[DME]_{9.6}[PF_6^-]$ and the resultant performance by varying other kinds of (c) solvent and (d-e) salt. ((b-e) Reproduced with permission of Ref. 85. Copyright 2020 American Chemical Society.) (f-g) Designed K^+ solvation structure, interfacial model, and performance of Sb anode. Exchange experiment of Sb anode electrode (h-i) from compatible to incompatible electrolyte and (j-k) from incompatible to compatible electrolyte. ((a, f-k) Reproduced with permission of Ref. 84. Copyright 2021 Wiley-VCH.) (color on line)

the Li^+-solvent-anion complex at the cathode interface and interprets the root cause of the varied performance in different electrolytes. For example, the battery employing different electrolytes of 1.0 mol·L^{-1} $LiPF_6$ in EMC, methyl acetate (MA), and MA/EMC (3:7, *V*/*V*) shows different performances (Figure 9b). It was found that the binding energy of Li^+-EMC is higher than that of Li^+-MA (Figure 9c), which leads to the higher de-solvation energy of the Li^+-EMC-PF_6^- complex (Figure 9d), in turn making the solvent-PF_6^- complex difficult to be de-solvated from the Li^+-solvent-PF_6^- and then keep far from the cathode interface. A cathode interfacial model can be constructed as below. In detail, in the electrolyte of 1.0 mol·L^{-1} $LiPF_6$ in EMC (i.e., $Li^+[EMC]_{8.11}[PF_6^-]$), the PF_6^- anion has a high frequency to appear around the Li^+ due to the low dielectric constant of EMC, then a strong interaction exists between the PF_6^- and Li^+ in the solvation structure (i.e., *f*1) and interfacial model (i.e., *f*1'). Then, the PF_6^- anion could be kept far from the cathode surface, as the Li^+ could neutralize the negative charge of the PF_6^- anion. This situation can mitigate the decomposition of PF_6^- anion on the cathode. In addition, as the PF_6^- cannot be close to the solvation structure on the cathode surface, the formed Li^+-EMC interaction accompanying the Li^+ de-intercalation is tight, which process can improve the antioxidant capacity of EMC (Figure 9e). In contrast, in the electrolyte of 1.0 mol·L^{-1} $LiPF_6$ in MA (i.e., $Li^+[MA]_{10.46}[PF_6^-]$), the PF_6^- anion can be kept far away from the Li^+ due to the high dielectric constant of MA, then a weak interaction exists between the PF_6^- and Li^+ in the solvation structure (i.e., *f*2) and interfacial model (i.e., *f*2'). Thus, the PF_6^--MA complex could get close to the cathode surface, as the Li^+ cannot neutralize the negative charge of PF_6^- anion effectively (Figure 9f). This situation can induce the decomposition of PF_6^--MA complex at the cathode interface, producing HF to corrode the cathode. In the electrolyte of 1.0 mol·L^{-1} $LiPF_6$ in EC/EMC (i.e., $Li^+[MA]_{3.14}[EMC]_{5.68}[PF_6^-]$), the PF_6^- anion appears around the Li^+ with a moderate frequency in the solvation structure (i.e., *f*3) and interfacial model (i.e., *f*3') (Figure 9g). In this way, an appropriate interaction can be formed between the PF_6^- anion and Li^+-solvent cluster, enabling the PF_6^- anion to keep a safe distance from the cathode side, in turn enhancing the anti-oxidation capability of PF_6^- anion.

Ming et al. also constructed the corresponding anode interfacial model (Figure 9h-j). In the EMC electrolyte, the Li^+ is difficult to be de-solvated from the Li^+-EMC-PF_6^- complex due to the high binding energy of Li^+-EMC and the low dielectric constant of EMC, where the resultant large polarization may lead to the Li dendrites growth on graphite. In the MA electrolyte, the MA solvent polarized by the Li^+ could be decomposed readily on the graphite due to the low electrochemical stability of MA. In MA/EMC electrolyte, the polarization of MA could be reduced significantly as the Li^+-EMC could dominate the interfacial model, which is similar to the role of EC in EC/EMC electrolyte as discussed before (Figure 4a, Figure 6f). Such arrangement of solvent molecules in the interfacial model implies that the electrochemical stability of MA could be much improved by the EMC. Meanwhile, the PF_6^- anion can also maintain a safe distance from the Li^+. In this case, the de-solvation energy of Li^+ is lower, thus Li^+ is more easily de-solvated and favors to be intercalated into the graphite anode, rather than forming the Li dendrites. By the muti-interactions of the cathode and anode interfacial models, the battery employing the MA/EMC electrolyte demonstrated higher performance. Note that this is the first time to construct interfacial model and study their interactions with the cathode interfacial model, this study opens a new avenue to build the relationship between the electrolyte interfacial model and electrode performance, besides the well-known SEI and CEI. This topic deserves more attention as it can guide the electrolyte design scientifically.

7 Conclusions and Perspectives

The importance of metal ion solvation structure and the derived interfacial model are emphasized in this review, which viewpoints differ from the SEI when we interpret the improved battery performance.

A scientific relationship between interfacial behavior (i.e., cation de-solvation process) and electrode performance, established by Ming's group, is a breakthrough in battery community, as more and more researchers have realized the critical role of the solvation structure and then put significant attention on the electrolyte researches since 2018[34]. However, this topic also becomes a controversial issue, as many researchers still believe that the SEI is critical to affect the electrode and battery performance. Thus, this is the reason why we would like to contribute this review entitled "which factor dominates battery performance: metal ion solvation structure-derived interfacial behaviors or solid electrolyte interphase?". We hope that more and more researches could contribute to the development of electrolytes, particularly, design more functional electrolytes, enabling the batteries to be operated with a long lifespan, non flammable, high-voltage, and/or wide-temperature features. But before that we have to admit that we have entered a new era of solvation structure and interfacial model, where the effect of SEI needs to be re-visited. The conventional electrolyte design, the SEI-based interpretation, may not be competent further, where we have to understand the relationship between the electrolyte behavior and electrode performance clearly at the molecular level for electrolyte design. Although the solvation structure and interfacial model have been validated in different electrode systems, they are mostly derived from experiments without specific theoretical support. The construction of these models in theory is a complex process that intersects multiple fields, such as the solution chemistry, solution-solid interface chemistry, calculation chemistry, physical chemistry, and organic chemistry at least. Thus, many scientific questions need to be solved when we promote the innovation of electrolytes, which are significant for the battery development practically.

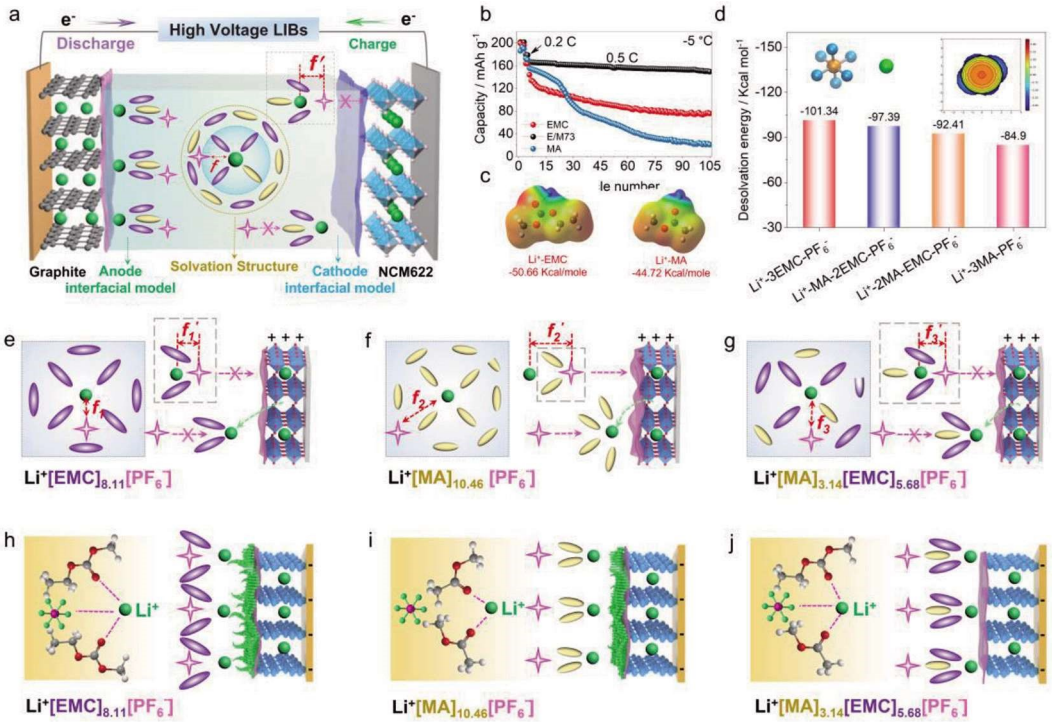

Figure 9 Designing electrolytes for full batteries by constructing cathode interfacial model. (a) Solvation structure and interfacial model of cathode and anode in graphite || NCM622 full battery. (b) Performance of battery by employing the designed electrolyte at −5 ℃ under 0.5 C. (c) Comparative binding energy of Li^+-EMC, Li^+-MA, and (d) de-solvation energy of Li^+-solvent-PF_6^- cluster. (e-g) Cathode interfacial model, (h-j) anode interfacial model and simulated electrolyte behaviors of $Li^+[EMC]_{8.11}[PF_6^-]$, $Li^+[MA]_{10.46}[PF_6^-]$ and $Li^+[MA]_{3.14}[EMC]_{5.68}[PF_6^-]$. ((a-j) Reproduced with permission of Ref. 90. Copyright 2022 Wiley-VCH.) (color on line)

i) Accuracy of the solvation structure and interface model. The parameters of the solvation structure including the geometry structure, binding energy, coordination number, interaction, and so on, need to be studied further. In addition, the interactions including the anion-solvent and/or solvent-solvent need to be considered further in the interfacial model, aiming to build a relationship with the electrolyte properties and electrode performances. Effective characterizations and analysis methods need to be developed.

ii) Characterizations of the de-solvation process at a molecular scale. The de-solvation process of solvation structure is a dynamic process that needs to be analyzed in conjunction with time-scale testing techniques. For example, the high spatiotemporal resolution electrochemical microscopy could be used to capture the molecular interfacial behaviors in the de-solvation processes. In addition, the arrangements of the cation, solvent, and anion in the interfacial model need to be quantified, particularly the variation upon the (dis-)charge process.

iii) Understanding the interaction between the cathode and anode interfacial models. The cathode interfacial model needs to pay more attention, as this kind of study is significant for designing electrolyte to stabilize the cathode, particularly at the high-voltage operations. The difference of molecular behaviors in the cathode and anode interfacial models also deserves to be investigated, as they can affect each other, in turn determining the battery performances.

iv) Discerning the influences of SEI and interfacial model. This is a topic about the interfacial chemistry and interphasial chemistry, which has become a mainstream and deserves more attention. More experiments need to be carried out to quantify the influences of SEI and the interfacial model. Note that different electrolytes and electrodes may have different conclusions, therefore, we have to figure out the common and difference.

Briefly, the metal ion solvation structure and the derived interfacial model provide new opportunities to understand the battery performance and guide the electrolyte design. The interfacial model can show the electrolyte behaviors on the molecular scale and build a relationship with the electrode performance. Moreover, this viewpoint deserves to be further studied in the aqueous batteries, which could be another view angle to understand the widened electrochemical stability window (ESW) and also the mitigated parasitic side reactions (e.g., hydrogen evolution reaction, etc.)[94]. We believe that these discoveries can contribute to development of electrolyte design and also complement the knowledge of the SEI in the battery community.

Acknowledgments:

The authors greatly thank the National Natural Science Foundation of China (22122904) for funding support. This work is also supported by the National Natural Science Foundation of China (21978281, 22109155). The authors also thank the bureau of international cooperation Chinese academy of sciences, CAS-NST Joint Research Projects (121522KYSB20200047), and the Scientific and Technological Developing Project of Jilin Province (YDZJ202101ZYTS022).

References:

[1] Li M, Lu J, Chen Z W, Amine K. 30 years of lithium-ion batteries[J]. Adv. Mater., 2018, 30(33): 1800561.

[2] Scrosati B, Hassoun J, Sun Y K. Lithium-ion batteries. A look into the future[J]. Energy Environ. Sci., 2011, 4(9): 3287-3295.

[3] Tarascon J M, Armand M. Issues and challenges facing rechargeable lithium batteries[J]. Nature, 2001, 414(6861): 359-367.

[4] Wu Y Q, Xie L Q, Ming H, Guo Y J, Hwang J Y, Wang W X, He X M, Wang L M, Alshareef H N, Sun Y K, Ming J. An empirical model for the design of batteries with high energy density[J]. ACS Energy Lett., 2020, 5(3): 807-816.

[5] Markevich E, Salitra G, Aurbach D. Fluoroethylene carbonate as an important component for the formation of an effective solid electrolyte interphase on anodes and cathodes for advanced Li-ion batteries[J]. ACS Energy Lett., 2017, 2(6): 1337-1345.

[6] Ruan D G, Chen M, Wen X Y, Li S Q, Zhou X G, Che Y X, Chen J K, Xiang W J, Li S L, Wang H, Liu X, Li W S. *In situ* constructing a stable interface film on high-voltage $LiCoO_2$ cathode via a novel electrolyte additive[J]. Nano

Energy, 2021, 90: 106535.

[7] Su C C, He M N, Cai M, Shi J Y, Amine R, Rago N D, Guo J C, Rojas T, Ngo A T, Amine K. Solvation-protection-enabled high-voltage electrolyte for lithium metal batteries[J]. Nano Energy, 2022, 92: 106720.

[8] Tan L J, Chen S Q, Chen Y W, Fan J J, Ruan D G, Nian Q S, Chen L, Jiao S H, Ren X D. Intrinsic nonflammable ether electrolytes for ultrahigh-voltage lithium metal batteries enabled by chlorine functionality[J]. Angew. Chem. Int. Edit., 2022, 61(32): e202203693.

[9] Xu K. Nonaqueous liquid electrolytes for lithium-based rechargeable batteries[J]. Chem. Rev., 2004, 104(10): 4303-4417.

[10] Mogi R, Inaba M, Jeong S K, Iriyama Y, Abe T, Ogumi Z. Effects of some organic additives on lithium deposition in propylene carbonate[J]. J. Electrochem. Soc., 2002, 149(12): A1578-A1583.

[11] Xu K. Electrolytes and interphases in Li-ion batteries and beyond[J]. Chem. Rev., 2014, 114(23): 11503-11618.

[12] Liang J Y, Zeng X X, Zhang X D, Wang P F, Ma J Y, Yin Y X, Wu X W, Guo Y G, Wan L J. Mitigating interfacial potential drop of cathode-solid electrolyte via ionic conductor layer to enhance interface dynamics for solid batteries[J]. J. Am. Chem. Soc., 2018, 140(22): 6767-6770.

[13] Wahyudi W, Cao Z, Kumar P, Li M L, Wu Y Q, Hedhili M N, Anthopoulos T D, Cavallo L, Li L J, Ming J. Phase inversion strategy to flexible freestanding electrode: Critical coupling of binders and electrolytes for high performance Li-S battery[J]. Adv. Funct. Mater., 2018, 28(34): 1802244.

[14] Fan J J, Dai P, Shi C G, Wen Y F, Luo C X, Yang J, Song C, Huang L, Sun S G. Synergistic dual-additive electrolyte for interphase modification to boost cyclability of layered cathode for sodium ion batteries[J]. Adv. Funct. Mater., 2021, 31(17): 2010500.

[15] Hou L P, Yao N, Xie J, Shi P, Sun S Y, Jin C B, Chen C M, Liu Q B, Li B Q, Zhang X Q, Zhang Q. Modification of nitrate ion enables stable solid electrolyte interphase in lithium metal batteries[J]. Angew. Chem. Int. Edit., 2022, 61(20): e202201406.

[16] Shin W, Manthiram A. A facile potential hold method for fostering an inorganic solid-electrolyte interphase for anode-free lithium-metal batteries[J]. Angew. Chem. Int. Edit., 2022, 61(13): e202115909.

[17] Xing L D, Zheng X W, Schroeder M, Alvarado J, Cresce A V, Xu K, Li Q S, Li W S. Deciphering the ethylene carbonate-propylene carbonate mystery in Li-ion batteries[J]. Acc. Chem. Res., 2018, 51(2): 282-289.

[18] Niu C J, Liu D Y, Lochala J A, Anderson C S, Cao X, Gross M E, Xu W, Zhang J G, Whittingham M S, Xiao J, Liu J. Balancing interfacial reactions to achieve long cycle life in high-energy lithium metal batteries[J]. Nature Energy, 2021, 6(7): 723-732.

[19] Shadike Z, Lee H, Borodin O, Cao X, Fan X L, Wang X L, Lin R Q, Bak S M, Ghose S, Xu K, Wang C S, Liu J, Xiao J, Yang X Q, Hu E Y. Identification of LiH and nanocrystalline LiF in the solid-electrolyte interphase of lithium metal anodes[J]. Nat. Nanotechnol., 2021, 16(5): 549-554.

[20] Kim M S, Zhang Z W, Rudnicki P E, Yu Z A, Wang J, Y Wang H S, Oyakhire S T, Chen Y L, Kim S C, Zhang W B, Boyle D T, Kong X, Xu R, Huang Z J, Huang W, Bent S F, Wang L W, Qin J, Bao Z N, Cui Y. Suspension electrolyte with modified Li^+ solvation environment for lithium metal batteries[J]. Nat. Mater., 2022, 21(4): 445-454.

[21] Wang H S, Yu Z, Kong X, Kim S C, Boyle D T, Qin J, Bao Z N, Cui Y. Liquid electrolyte: The nexus of practical lithium metal batteries[J]. Joule, 2022, 6(3): 588-616.

[22] Fong R, Vonsacken U, Dahn J R. Studies of lithium intercalation into carbons using nonaqueous electrochemical cells[J]. J. Electrochem. Soc., 1990, 137(7): 2009-2013.

[23] Cheng M, Tang W P, Li Y, Zhu K J. Study on compositions and changes of SEI-film of Li_2MnO_3 positive material during the cycles[J]. Catal. Today, 2016, 274: 116-122.

[24] Hope M A, Rinkel B L D, Gunnarsdottir A B, Marker K, Menkin S, Paul S, Sergeyev I V, Grey C P. Selective NMR observation of the SEI-metal interface by dynamic nuclear polarisation from lithium metal[J]. Nat. Commun., 2020, 11(1): 2224.

[25] Zhao F P, Zhang S M, Li Y G, Sun X L. Emerging characterization techniques for electrode interfaces in sulfide-based all-solid-state lithium batteries[J]. Small Structures, 2021, 3(1): 2100146.

[26] Zhou Y F, Su M, Yu X F, Zhang Y Y, Wang J G, Ren X D, Cao R G, Xu W, Baer D R, Du Y G, Borodin O, Wang Y T, Wang X L, Xu K, Xu Z J, Wang C M, Zhu Z H. Real-time mass spectrometric characterization of the solid-electrolyte interphase of a lithium-ion battery [J]. Nat. Nanotechnol., 2020, 15(3): 224-230.

[27] Andersson A M, Henningson A, Siegbahn H, Jansson U, Edström K. Electrochemically lithiated graphite characterised by photoelectron spectroscopy[J]. J. Power Sources, 2003, 119: 522-527.

[28] Lu P, Harris S J. Lithium transport within the solid electrolyte interphase[J]. Electrochem. Commun., 2011, 13

(10): 1035-1037.

[29] Xu H Y, Li Z P, Liu T C, Han C, Guo C, Zhao H, Li Q, Lu J, Amine K, Qiu X P. Impacts of dissolved Ni^{2+} on the solid electrolyte interphase on a graphite anode[J]. Angew. Chem. Int. Edit., 2022, 61(30): e202202894.

[30] Li Y Z, Li Y B, Pei A L, Yan K, Sun Y M, Wu C L, Joubert L M, Chin R, Koh A L, Yu Y, Perrino J, Butz B, Chu S, Cui Y. Atomic structure of sensitive battery materials and interfaces revealed by cryo-electron microscopy [J]. Science, 2017, 358(6362): 506-510.

[31] Zhang Z W, Li Y Z, Xu R, Zhou W J, Li Y B, Oyakhire S T, Wu Y C, Xu J W, Wang H S, Yu Z A, Boyle D T, Huang W, Ye Y S, Chen H, Wan J Y, Bao Z N, Chiu W, Cui Y. Capturing the swelling of solid-electrolyte interphase in lithium metal batteries[J]. Science, 2022, 375 (6576): 66-70.

[32] Cheng H R, Sun Q J, Li L L, Zou Y G, Wang Y Q, Cai T, Zhao F, Liu G, Ma Z, Wahyudi W, Li Q, Ming J. Emerging era of electrolyte solvation structure and interfacial model in batteries[J]. ACS Energy Lett., 2022, 7(1): 490-513.

[33] Ming J, Cao Z, Wahyudi W, Li M L, Kumar P, Wu Y Q, Hwang J Y, Hedhili M N, Cavallo L, Sun Y K, Li L J. New insights on graphite anode stability in rechargeable batteries: Li ion coordination structures prevail over solid electrolyte interphases[J]. ACS Energy Lett., 2018, 3(2): 335-340.

[34] Ming J, Cao Z, Wu Y Q, Wahyudi W, Wang W X, Guo X R, Cavallo L, Hwang J Y, Shamim A, Li L J, Sun Y K, Alshareef H N. New insight on the role of electrolyte additives in rechargeable lithium ion batteries[J]. ACS Energy Lett., 2019, 4(11): 2613-2622.

[35] Jeong S K, Inaba M, Iriyama Y, Abe T, Ogumi Z. Electrochemical intercalation of lithium ion within graphite from propylene carbonate solutions[J]. Electrochem. Solid State Lett., 2003, 6(1): A13-A15.

[36] Xu K. "Charge-transfer" process at graphite/electrolyte interface and the solvation sheath structure of Li^+ in nonaqueous electrolytes[J]. J. Electrochem. Soc., 2007, 154 (3): A162-A167.

[37] Yamada Y, Yaegashi M, Abe T, Yamada A. A superconcentrated ether electrolyte for fast-charging Li-ion batteries[J]. Chem. Commun., 2013, 49(95): 11194-11196.

[38] Yamada Y, Furukawa K, Sodeyama K, Kikuchi K, Yaegashi M, Tateyama Y, Yamada A. Unusual stability of acetonitrile-based superconcentrated electrolytes for fast-charging lithium-ion batteries[J]. J. Am. Chem. Soc., 2014, 136(13): 5039-5046.

[39] Ren X D, Gao P Y, Zou L F, Jiao S H, Cao X, Zhang X H, Jia H, Engelhard M H, Matthews B E, Wu H P, Lee H, Niu C J, Wang C M, Arey B W, Xiao J, Liu J, Zhang J G, Xu W. Role of inner solvation sheath within salt-solvent complexes in tailoring electrode/electrolyte interphases for lithium metal batteries[J]. Proc. Natl. Acad. Sci. U.S.A., 2020, 117(46): 28603-28613.

[40] Cao X, Gao P Y, Ren X D, Zou L F, Engelhard M H, Matthews B E, Hu J T, Niu C J, Liu D Y, Arey B W, Wang C M, Xiao J, Liu J, Xu W, Zhang J G. Effects of fluorinated solvents on electrolyte solvation structures and electrode/electrolyte interphases for lithium metal batteries[J]. Proc. Natl. Acad. Sci. U.S.A., 2021, 118(9): e2020357118.

[41] Liu G, Sun Q J, Li Q, Zhang J L, Ming J. Electrolyte issues in lithium-sulfur batteries: Development, prospect, and challenges[J]. Energy & Fuels, 2021, 35(13): 10405-10427.

[42] Sun Q J, Cao Z, Zhang J L, Cheng H R, Zhang J, Li Q, Ming H, Liu G, Ming J. Metal catalyst to construct carbon nanotubes networks on metal oxide microparticles towards designing high-performance electrode for high-voltage lithium-ion batteries[J]. Adv. Funct. Mater., 2021, 31(22): 2009122.

[43] Wahyudi W, Ladelta V, Tsetseris L, Alsabban M M, Guo X R, Yengel E, Faber H, Adilbekova B, Seitkhan A, Emwas A H, Hedhili M N, Li L J, Tung V, Hadjichristidis N, Anthopoulos T D, Ming J. Lithium-ion desolvation induced by nitrate additives reveals new insights into high performance lithium batteries[J]. Adv. Funct. Mater., 2021, 31(23): 2101593.

[44] Liu G, Cao Z, Wang P, Ma Z, Zou Y G, Sun Q J, Cheng H R, Cavallo L, Li S Y, Li Q, Ming J. Switching electrolyte interfacial model to engineer solid electrolyte interface for fast charging and wide-temperature lithium-ion batteries[J]. Adv. Sci., 2022, 9(26): 2201893.

[45] Tian Z N, Zou Y G, Liu G, Wang Y Z, Yin J, Ming J, Alshareef H N. Electrolyte solvation structure design for sodium ion batteries[J]. Adv. Sci., 2022, 9(22): 2201207.

[46] Wahyudi W, Guo X R, Ladelta V, Tsetseris L, Nugraha M I, Lin Y B, Tung V, Hadjichristidis N, Li Q, Xu K, Ming J, Anthopoulos T D. Hitherto unknown solvent and anion pairs in solvation structures reveal new insights into high-performance lithium-ion batteries[J]. Adv. Sci., 2022, 9(28): 2202405.

[47] Chen S R, Zheng J M, Mei D H, Han K S, Engelhard M H, Zhao W G, Xu W, Liu J, Zhang J G. High-voltage lithium-metal batteries enabled by localized high-concen-

tration electrolytes[J]. Adv. Mater., 2018, 30(21): 1706102.

[48] Chen S R, Zheng J M, Yu L, Ren X D, Engelhard M H, Niu C J, Lee H, Xu W, Xiao J, Liu J, Zhang J G. High-efficiency lithium metal batteries with fire-retardant electrolytes[J]. Joule, 2018, 2(8): 1548-1558.

[49] Deng W, Dai W H, Zhou X F, Han Q G, Fang W, Dong N, He B Y, Liu Z P. Competitive solvation-induced concurrent protection on the anode and cathode toward a 400 $Wh\cdot kg^{-1}$ lithium metal battery[J]. ACS Energy Lett., 2021, 6(1): 115-123.

[50] Jie Y L, Liu X J, Lei Z W, Wang S Y, Chen Y W, Huang F Y, Cao R G, Zhang G Q, Jiao S H. Enabling high-voltage lithium metal batteries by manipulating solvation structure in ester electrolyte[J]. Angew. Chem. Int. Edit., 2020, 59(9): 3505-3510.

[51] Jiang L L, Yan C, Yao Y X, Cai W L, Huang J Q, Zhang Q. Inhibiting solvent co-intercalation in a graphite anode by a localized high-concentration electrolyte in fast-charging batteries[J]. Angew. Chem. Int. Edit., 2021, 60(7): 3402-3406.

[52] Li F, He J, Liu J D, Wu M G, Hou Y Y, Wang H P, Qi S H, Liu Q H, Hu J W, Ma J M. Gradient solid electrolyte interphase and lithium-ion solvation regulated by bisfluoroacetamide for stable lithium metal batteries[J]. Angew. Chem. Int. Edit., 2021, 60(12): 6600-6608.

[53] Ming J, Cao Z, Li Q, Wahyudi W, Wang W X, Cavallo L, Park K J, Sun Y K, Alshareef H N. Molecular-scale interfacial model for predicting electrode performance in rechargeable batteries[J]. ACS Energy Lett., 2019, 4(7): 1584-1593.

[54] Xu K, Lee U, Zhang S S, Jow T R. Graphite/electrolyte interface formed in LiBOB-based electrolytes-II. Potential dependence of surface chemistry on graphitic anodes [J]. J. Electrochem. Soc., 2004, 151(12): A2106-A2112.

[55] Yao W H, Zhang Z R, Gao J, Li J, Xu J, Wang Z C, Yang Y. Vinyl ethylene sulfite as a new additive in propylene carbonate-based electrolyte for lithium ion batteries [J]. Energy Environ. Sci., 2009, 2(10): 1102-1108.

[56] Nie M Y, Chalasani D, Abraham D P, Chen Y J, Bose A, Lucht B L. Lithium ion battery graphite solid electrolyte interphase revealed by microscopy and spectroscopy [J]. J. Phys. Chem. C, 2013, 117(3): 1257-1267.

[57] Ping P, Xia X, Wang Q S, Sun J H, Dahn J R. The effect of trimethoxyboroxine on some positive electrodes for Li-ion batteries[J]. J. Electrochem. Soc., 2013, 160(3): A426-A429.

[58] Peled E. The electrochemical behavior of alkali and alkaline earth metals in nonaqueous battery systems-the solid electrolyte interphase model[J]. J. Electrochem. Soc., 1979, 126(12): 2047-2051.

[59] Peled E. Film forming reaction at the lithium/electrolyte interface[J]. J. Power Sources, 1983, 9(3-4): 253-266.

[60] Peled E, Golodnitsky D, Ardel G. Advanced model for solid electrolyte interphase electrodes in liquid and polymer electrolytes[J]. J. Electrochem. Soc., 1997, 144(8): L208-L210.

[61] Goodenough J B, Kim Y. Challenges for rechargeable Li batteries[J]. Chem. Mater., 2010, 22: 587-603.

[62] Aurbach D, Levi M D, Levi E, Schechter A. Failure and stabilization mechanisms of graphite electrodes[J]. J. Phys. Chem. B, 1997, 101(12): 2195-2206.

[63] Li T, Balbuena P B. Theoretical studies of the reduction of ethylene carbonate [J]. Chem. Phys. Lett, 2000, 317 (3-5): 421-429.

[64] Aurbach D, Gamolsky K, Markovsky B, Gofer Y, Schmidt M, Heider U. On the use of vinylene carbonate (VC) as an additive to electrolyte solutions for Li-ion batteries[J]. Electrochim. Acta, 2002, 47(9): 1423-1439.

[65] Edström K, Gustafsson T, Thomas J O. The cathode-electrolyte interface in the Li-ion battery[J]. Electrochim. Acta, 2004, 50(2-3): 397-403.

[66] Blyth R I R, Buqa H, Netzer F P, Ramsey M G, Besenhard J O, Golob P, Winter M. XPS studies of graphite electrode materials for lithium ion batteries[J]. Appl. Surf. Sci., 2000, 167(1-2): 99-106.

[67] Yang G, Ivanov I N, Ruther R E, Sacci R L, Subjakova V, Hallinan D T, Nanda J. Electrolyte solvation structure at solid-liquid interface probed by nanogap surface-enhanced Raman spectroscopy[J]. ACS Nano, 2018, 12(10): 10159-10170.

[68] Zhang S S. A review on electrolyte additives for lithium-ion batteries[J]. J. Power Sources, 2006, 162(2): 1379-1394.

[69] Li W Y, Yao H B, Yan K, Zheng G Y, Liang Z, Chiang Y M, Cui Y. The synergetic effect of lithium polysulfide and lithium nitrate to prevent lithium dendrite growth[J]. Nat. Commun., 2015, 6: 7436.

[70] Haregewoin A M, Wotango A S, Hwang B J. Electrolyte additives for lithium ion battery electrodes: Progress and perspectives[J]. Energy Environ. Sci., 2016, 9(6): 1955-1988.

[71] Xia J, Dahn J R. Improving sulfolane-based electrolyte for high voltage Li-ion cells with electrolyte additives[J]. J. Power Sources, 2016, 324: 704-711.

[72] Xia J, Nelson K J, Lu Z H, Dahn J R. Impact of electrolyte solvent and additive choices on high voltage

Li-ion pouch cells[J]. J. Power Sources, 2016, 329: 387-397.

[73] Zheng J M, Engelhard M H, Mei D H, Jiao S H, Polzin B J, Zhang J G, Xu W. Electrolyte additive enabled fast charging and stable cycling lithium metal batteries [J]. Nature Energy, 2017, 2(3): 17012.

[74] Wang X S, Mai W C, Guan X C, Liu Q, Tu W Q, Li W S, Kang F Y, Li B H. Recent advances of electroplating additives enabling lithium metal anodes to applicable battery techniques[J]. Energy Environ. Mater., 2020, 4(3): 284-292.

[75] Yamada Y, Koyama Y, Abe T, Ogumi Z. Correlation between charge-discharge behavior of graphite and solvation structure of the lithium ion in propylene carbonate-containing electrolytes[J]. J. Phys. Chem. C, 2009, 113 (20): 8948-8953.

[76] Yamada Y, Takazawa Y, Miyazaki K, Abe T. Electrochemical lithium intercalation into graphite in dimethyl sulfoxide-based electrolytes: Effect of solvation structure of lithium ion[J]. J. Phys. Chem. C, 2010, 114(26): 11680-11685.

[77] Jiang L L, Yan C, Yao Y X, Cai W L, Huang J Q, Zhang Q. Inhibiting solvent co-intercalation in a graphite anode by a localized high-concentration electrolyte in fast-charging batteries[J]. Angew. Chem. Int. Ed. Engl., 2021, 60(7): 3402-3406.

[78] Zhang J, Cao Z, Zhou L, Liu G, Park G T, Cavallo L, Wang L M, Alshareef H N, Sun Y K, Ming J. Model-based design of graphite-compatible electrolytes in potassium-ion batteries[J]. ACS Energy Lett., 2020, 5(8): 2651-2661.

[79] Liu G, Cao Z, Zhou L, Zhang J, Sun Q J, Hwang J Y, Cavallo L, Wang L M, Sun Y K, Ming J. Additives engineered nonflammable electrolyte for safer potassium ion batteries[J]. Adv. Funct. Mater., 2020, 30(43): 2001934.

[80] Li Q, Cao Z, Liu G, Cheng H R, Wu Y Q, Ming H, Park G T, Yin D M, Wang L M, Cavallo L, Sun Y K, Ming J. Electrolyte chemistry in 3D metal oxide nanorod arrays deciphers lithium dendrite-free plating/stripping behaviors for high-performance lithium batteries[J]. J. Phys. Chem. Lett., 2021, 12(20): 4857-4866.

[81] Li Q, Cao Z, Wahyudi W, Liu G, Park G T, Cavallo L, Anthopoulos T D, Wang L M, Sun Y K, Alshareef H N, Ming J. Unraveling the new role of an ethylene carbonate solvation shell in rechargeable metal ion batteries[J]. ACS Energy Lett., 2021, 6(1): 69-78.

[82] Zhang J, Cao Z, Zhou L, Park G T, Cavallo L, Wang L M, Alshareef H N, Sun Y K, Ming J. Model-based design of stable electrolytes for potassium ion batteries[J]. ACS Energy Lett., 2020, 5(10): 3124-3131.

[83] Zhou L, Cao Z, Zhang J, Sun Q J, Wu Y Q, Wahyudi W, Hwang J Y, Wang L M, Cavallo L, Sun Y K, Alshareef H N, Ming J. Engineering sodium-ion solvation structure to stabilize sodium anodes: Universal strategy for fast-charging and safer sodium-ion batteries[J]. Nano Lett., 2020, 20(5): 3247-3254.

[84] Zhou L, Cao Z, Zhang J, Cheng H R, Liu G, Park G T, Cavallo L, Wang L M, Alshareef H N, Sun Y K, Ming J. Electrolyte-mediated stabilization of high-capacity micro-sized antimony anodes for potassium-ion batteries[J]. Adv. Mater., 2021, 33(8): 2005993.

[85] Zhou L, Cao Z, Wahyudi W, Zhang J, Hwang J Y, Cheng Y, Wang L M, Cavallo L, Anthopoulos T, Sun Y K, Alshareef H N, Ming J. Electrolyte engineering enables high stability and capacity alloying anodes for sodium and potassium ion batteries[J]. ACS Energy Lett., 2020, 5 (3): 766-776.

[86] Sun Q J, Cao Z, Ma Z, Zhang J L, Cheng H R, Guo X R, Park G T, Li Q, Xie E Q, Cavallo L, Sun Y-K, Ming J. Dipole-dipole interaction induced electrolyte interfacial model to stabilize antimony anode for high-safety lithium-ion batteries[J]. ACS Energy Lett., 2022, 7(10): 3545-3556.

[87] Sun Q J, Cao Z, Ma Z, Zhang J L, Wahyudi W, Cai T, Cheng H R, Li Q, Kim H, Xie E Q, Cavallo L, Sun Y K, Ming J. Discerning roles of interfacial model and solid electrolyte interphase layer for stabilizing antimony anode in lithium-ion batteries[J]. ACS Materials Lett., 2022, 4(11): 2233-2243.

[88] Sun Q J, Cao Z, Ma Z, Zhang J L, Wahyudi W, Liu G, Cheng H R, Cai T, Xie E Q, Cavallo L, Li Q, Ming J. Interfacial and interphasial chemistry of electrolyte components to invoke high-performance antimony anodes and non-flammable lithium-ion batteries[J]. Adv. Funct. Mater., doi: 10.1002/adfm.202210292.

[89] Zou Y G, Shen Y B, Wu Y Q, Xue H J, Guo Y J, Liu G, Wang L M, Ming J. A designed durable electrolyte for high-voltage lithium-ion batteries and mechanism analysis[J]. Chem.-Eur. J., 2020, 26(35): 7930-7936.

[90] Liao X L, Huang Q M, Mai S W, Wang X S, Xu M Q, Xing L D, Liao Y H, Li W S. Self-discharge suppression of 4.9 V $LiNi_{0.5}Mn_{1.5}O_4$ cathode by using tris(trimethylsilyl)borate as an electrolyte additive[J]. J. Power Sources, 2014, 272: 501-507.

[91] Röser S, Lerchen A, Ibing L, Cao X, Kasnatscheew J, Glorius F, Winter M, Wagner R. Highly effective solid

electrolyte interphase-formin g electrolyte additive enabling high voltage lithium-ion batteries[J]. Chem. Mater., 2017, 29(18): 7733-7739.

[92] Ma L, Ellis L, Glazier S L, Ma X W, Liu Q Q, Li J, Dahn J R. $LiPO_2F_2$ as an electrolyte additive in $Li[Ni_{0.5}Mn_{0.3}Co_{0.2}]O_2$/graphite pouch cells[J]. J. Electrochem. Soc., 2018, 165 (5): A891-A899.

[93] Zou Y G, Cao Z, Zhang J, Wahyudi W, Wu Y Q, Liu G, Li Q, Cheng H R, Zhang D Y, Park G T, Cavallo L, Anthopoulos T D, Wang L M, Sun Y K, Ming J. Interfacial model deciphering high-voltage electrolytes for high energy density, high safety, and fast-charging lithium-ion batteries[J]. Adv. Mater., 2021, 33(43): 2102964.

[94] Ming J, Guo J, Xia C, Wang W X, Alshareef H N. Zinc-ion batteries: materials, mechanisms, and applications[J]. Mat. Sci. Eng. R., 2019, 135: 58-84.

影响电池性能的因素:金属离子溶剂化结构衍生的界面行为还是固体电解质界面膜?

程浩然[1,2],马 征[1],郭营军[3],孙春胜[3],李 茜[1],明 军[1,2*]

(1. 中国科学院长春应用化学研究所稀土资源利用国家重点实验室, 吉林 长春 130022; 2. 中国科学技术大学应用化学与工程学院, 安徽 合肥 230026; 3. 湖州昆仑亿恩科电池材料有限公司, 浙江 湖州 313103)

摘要: 通过电解液分解在电极上形成的固体电解质界面(SEI)层被认为是影响电池性能的最重要因素。然而,我们发现金属离子溶剂化结构也会影响其电极性能,尤其可以阐明许多 SEI 无法解释的实验现象。基于该综述,本文总结了金属离子溶剂化结构和衍生的金属离子去溶剂化行为的重要性,并建立了相应的界面模型以展示界面行为和电极性能之间的关系,并将其应用于不同的电极和电池体系。我们强调了电极界面离子/分子相互作用对电极性能的影响,该解释与以往基于 SEI 的解释不同。该综述为理解电池性能和指导电解液设计提供了一个新的视角。

关键词: 电池;电解液;溶剂化结构;电极界面模型;固体电解质界面膜